



IAEA

International Atomic Energy Agency

INDC(NDS)-0778

Distr. AC

INDC International Nuclear Data Committee

The Importance of Resonance Self-Shielding

Dermott E. Cullen

1466 Hudson Way, Livermore, CA94550, U.S.A

March 2019

IAEA Nuclear Data Section

Vienna International Centre, P.O. Box 100, 1400 Vienna, Austria

Selected INDC documents may be downloaded in electronic form from
<http://www-nds.iaea.org/publications>
or sent as an e-mail attachment.

Requests for hardcopy or e-mail transmittal should be directed to
NDS.Contact-Point@iaea.org

or to:

Nuclear Data Section
International Atomic Energy Agency
Vienna International Centre
PO Box 100
1400 Vienna
Austria

Printed by the IAEA in Austria

March 2019

The Importance of Resonance Self-Shielding

Dermott E. Cullen
1466 Hudson Way, Livermore, CA94550, U.S.A

March 2019

Contents

| | |
|--|----|
| Overview | 7 |
| The Multi-Group Problem | 8 |
| Spatial Zoning..... | 10 |
| Cross Sections versus Distance of Collision | 11 |
| Six Cross Section Models..... | 11 |
| Definition of Criticality | 12 |
| Simple, 1-D, Planar Example | 13 |
| Flux, Reactions and Average Total Cross Section vs. Depth into Uranium | 17 |
| Transmission Measurements | 28 |
| Statistics | 29 |
| 311 U-235 Slow Critical Assemblies | 31 |
| Is it the model or Statistics? | 34 |
| Boundary Conditions..... | 39 |
| Infinite and Homogeneous | 41 |
| The Unresolved Resonance Region..... | 43 |
| Conclusions | 45 |
| Acknowledgment | 46 |
| References | 46 |
| APPENDICES | 48 |
| A Long History of Time | 48 |
| A Brief History of Time | 49 |
| Probability Table versus Multi-Band Methods | 50 |
| Bondarenko Model | 53 |
| The Intermediate Resonance (IR) Approximation | 56 |

Overview

In this paper I describe why Resonance Self-Shielding is so important, and I present examples to illustrate the magnitude of this effect. More importantly, in order to improve the accuracy of our results, I address what can be done to improve our treatment of self-shielding. Throughout I use recent ENDF data [1, 2], and Monte Carlo codes TART [3], and MCNP [4].

I point out the difference between Monte Carlo and deterministic codes (e.g., Sn), as it relates to how each treats self-shielding; particularly with regard to boundary conditions. Self-shielding means using energy averaged cross sections: obviously this applies to multi-group codes, but it also applies even to codes that use continuous energy cross sections [3, 4], to correctly include self-shielding in the unresolved resonance region [5, 6].

Lastly, I address the question of the statistical accuracy of Monte Carlo codes, and I present numerous examples, both very simple theoretical results, and hundreds of critical assemblies.

Please note that today our computers are fast enough and large enough that for my own applications with my TART Monte Carlo code [3], I always use continuous energy cross sections, not multi-group. Therefore, self-shielding is no longer a problem I must deal with, except in the unresolved resonance region [5, 6], where an “energy average” statistical approach is still required and used by both TART [3], and MCNP [4], see the appendix for details.

My conclusions include,

- 1) Failure to account for resonance self-shielding can give RUBBISH results. When you use unshielded cross sections be aware: **The results from any computer code can be no better than the data they use**; with unshielded cross sections you can be in a: garbage in, garbage out, situation.
- 2) Standard methods of self-shielding in principle only apply to infinite, homogeneous media, but in practice they produce surprisingly accurate results for integral parameters, such as k_{eff} . However, they fail to accurately account for important spatial and directional results simultaneously for thick and thin media, such as spatially dependent fuel burn-up.
- 3) The multi-band method is designed to accurately reproduce both integral parameters, such as k_{eff} , as well as spatial and directional results, for media which are optically thick or thin media (multi-group does not), and generally agrees with results based on using continuous energy cross sections.

The multi-band method as used by TART [3] is used at all energies, whereas with MCNP [4], it has only been applied to self-shielding in the unresolved energy range. The multi-band method owes much to the earlier work of Nikolaev [23] and Levitt [24, 25]; it differs in providing an analytical solution to the multi-band equations, to explicitly conserve expected moments of the flux and reaction rates, and in using Monte Carlo [3], to make practical the correct, all important, boundary conditions, ala Nikolaev’s all the way approach [23]. The results included in this report are based on using the multi-band method in the TART Monte Carlo code [3] for over 40 years, during which time it has been applied to thousands of applications.

The Multi-Group Problem

The problem with the Multi-Group method is that we have to “guess” the answer, in order to define the multi-group constants, and our “guess”, even when using many groups (here I use 616 groups), can have a major impact on the accuracy of our answers.

Let’s look at the source of the problem. The following applies to any geometry, but for simplicity, I will illustrate results starting from the time independent, linear transport equation, in planar geometry with continuous energy, and I will then explicitly describe the six models I used for the **continuous, multi-group** and **multi-band** cross sections,

$$\mu \partial \Phi(E, z, \mu) / \partial z + \Sigma_t(E, z) * \Phi(E, z, \mu) = R(E, z, \mu) \text{ is the slowing down and sources.}$$

The multi-group equations are obtained by integrating over adjacent energy ranges, and usually spatial regions, and direction, to define multi-group constants,

$$\mu \partial \langle \Phi(E, z, \mu) dE \rangle / \partial z + \langle \Sigma_t(E, z) * \Phi(E, z, \mu) dE \rangle = \langle R(E, z, \mu) dE \rangle, \text{ or, equivalently,}$$

$$\mu \partial \Phi_g(z, \mu) / \partial z + \Sigma_{tg}(z) * \Phi_g(z, \mu) = Rg(z, \mu)$$

Where the group averaged total cross section is defined as **the group averaged ratio of reactions to flux,**

$$\Sigma_{tg}(z) = \frac{\langle \Sigma_t(E, z) * \Phi(E, z, \mu) dE \rangle}{\langle \Phi(E, z, \mu) dE \rangle} = \frac{\text{Reactions}}{\text{Flux}}$$

Our problem is that in order to define our multi-group cross sections, $\Sigma_{tg}(z)$, we must “guess” at the **energy dependence** of the flux, $\Phi(E, z, \mu)$, which is the answer we are trying to find; sounds like a “Catch-22” situation. Less obvious we are integrating not only over energy, but usually **also over space and direction**. Generally, the energy dependent flux can be approximated by the product of two terms: **an energy dependent spectrum**, e.g., Maxwellian at low energy, $1/E$ in the slowing down range, and a fission and even possibly fusion source at higher energies, and **a cross section dependent**, self-shielding factor. For the slowing down here, I assume it is “smooth” in energy, which implies the **narrow resonance (NR)** approximation (an additional complication I will not address here). For a sufficiently large number of groups the assumption of the energy dependent term plays only a minor role, and since it appears in both numerator and denominator **its normalization plays no role at all**.

Unfortunately, the same cannot be said about the cross section dependent self-shielding factor. Here the effect is persistent for even many groups, indeed it plays a role as long as the width of a group is large compared to the width of resonances in the total cross section. We can see this by returning to our original energy dependent equation and assuming,

$\Phi(E, z, \mu) \sim \Phi(E, \mu) * \text{Exp}[K * z]$, similar to a Laplace transform or Case method

$$\{\mu K + \Sigma_t(E, z)\} \Phi(E, \mu) = R(E, \mu)$$

$$\Phi(E, \mu) = \frac{R(E)}{\{\mu K + \Sigma_t(E, z)\}} ; \text{ here } R(E) \text{ is an energy dependent term (no angular dependence)}$$

; here the denominator is the self-shielding factor

We can see here that neutron flux is inversely related to the total cross section, plus a spatially and direction dependent term, μK . One interpretation of the flux (the interpretation we use in our Monte Carlo codes) is that the flux is the distance travelled by the neutrons normalized per unit time, space, energy and direction; which helps us understand the above inverse relationship to the total cross section, e.g., doubling the total cross section will half the distance travelled by the neutrons, and hence half the flux. **This is referred to as “self-shielding” because it is the variation in the total cross section, itself, that causes variation in the flux;** it is this flux that we want to calculate using our multi-group equations, but as we can see here it is also the flux that we must “guess” in order to define our multi-group constants.

The most commonly used self-shielding models start from our above equation, and assume we have an **infinite, homogeneous** medium, i.e., ignore the μK term,

$$\Phi(E) = \frac{R(E)}{\{\Sigma_t(E, z)\}} ; \text{ note, here I have omitted the directional dependence of flux, } \Phi(E)$$

An additional complication is that here the total cross section in the denominator is not the total of each evaluation (which is application independent), but rather the total of whatever mix of materials we are using in each spatial zone we are averaging over (obviously application dependent). Historically due to limited computer resources we wanted to only define application independent multi-group libraries, so another approximation is introduced; the **Bondarenko**, or partial shielding, where we assume that the total cross section for any mixture can be defined as that of each evaluation, plus a second cross section, Σ_0 , which can be any value between zero (Totally Shielded) to infinity (Unshielded or infinitely dilute), cross sections,

$$\Sigma_{tg}(z) = \frac{\langle \Sigma_t(E, z) * R(E) \text{ dE} / \{\Sigma_t(E, z) + \Sigma_0\} \text{ dE} \rangle}{\langle R(E) \text{ dE} / \{\Sigma_t(E, z) + \Sigma_0\} \text{ dE} \rangle} ; \Sigma_{tg}(z) \text{ constant within spatial zone (z)}$$

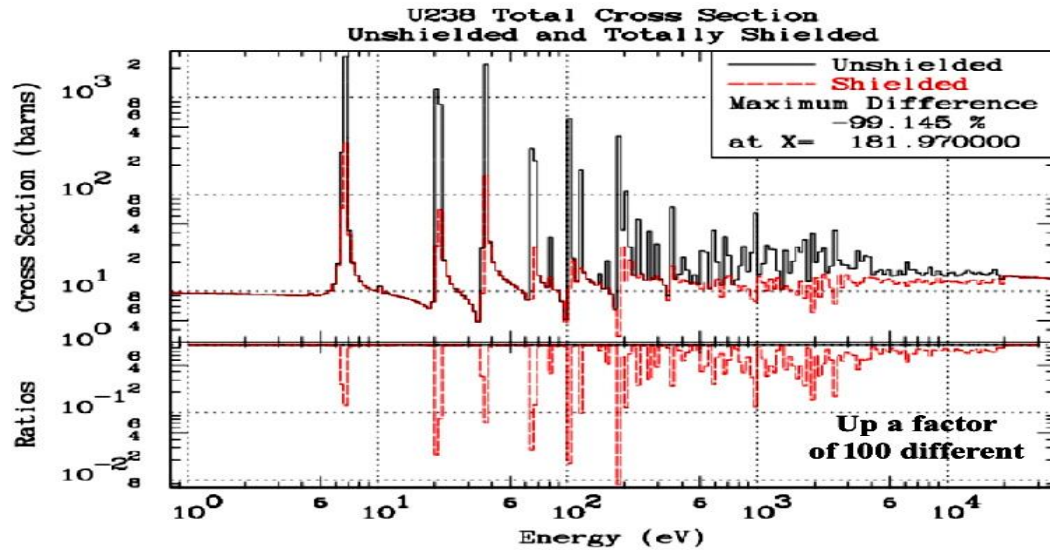
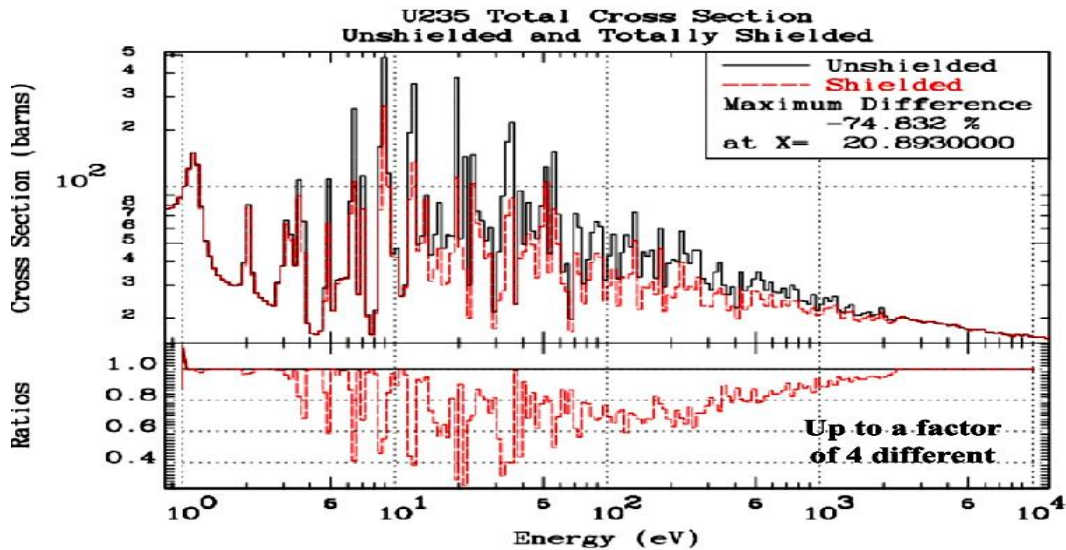
Let's review the explicit approximations used to arrive at this equation,

- 1) Infinite, Homogeneous media; ignore μK .
- 2) Narrow resonances, which affects the slowing down spectrum, $R(E)$.
- 3) Resonance structure in each evaluation independent; $\Sigma_t(E, z) + \Sigma_0$

In addition, there are less obvious implied approximations

- 1) Multi-group constants are constant throughout each spatial region
- 2) Multi-group constants are independent of direction

The below plots illustrate the ^{235}U and ^{238}U Total Cross Section using the TART 616 group structure (50 groups per energy decade from 10^{-5} eV to 20 MeV), comparing Unshielded and Totally Shielded cross sections. These plots illustrate that even with 616 groups, the ^{235}U Shielded Total can be up to $\sim 75\%$ less than the Unshielded (i.e., 1/4-th of it), and for ^{238}U it can be over 99% less (100 times less). **So the differences due to self-shielding can be ENORMOUS; increasing to 2,020 groups does not improve things by much.**



Spatial Zoning

One very important point to note: if a region of space contains only one mixture of materials, dividing this region into smaller and smaller volumes has no effect on these self-shielding models, so regardless of how fine we zone our geometry, this will not change the results shown below.

Cross Sections versus Distance of Collision

Note that above I only mention calculating the cross section, but in our Monte Carlo codes we sample the distance to collision, not the total cross section,

$$\text{Distance} = -\log(\text{random}) / \Sigma t(E,z)$$

Here we are trying to estimate the flux = the distance travelled by the neutrons. This suggests also that when we estimate the flux used as weighting in our multi-group equations, it should also be the distance to collision, or the inverse of the total cross sections, as shown in the above equations.

Six Cross Section Models

To illustrate the importance of self-shielding, I will use six different cross section models that I have included in the TART Monte Carlo code [3]. All the below differences shown for the simple 1-D planar, and 311 Slow Uranium problems are due solely to how these approximations are used in the six cross sections models; these six models include,

- 1) **Continuous** Energy Cross sections [7, 8], including Multi-Band shielding in the unresolved – this has the fewest approximations and here I assume produces the most accurate results to which all others are compared.
- 2) **Multi-Band** Cross Sections at ALL energies – uses the fewer approximations (as will be explained in detail below), and in this study it consistently produces results that agree closely with the Continuous energy results.
- 3) **Multi-Group** Cross Sections at ALL energies (unshielded energy averages) – this model completely ignores self-shielding and defines group averages by merely integrating over the energy range of each group,
 $\Phi(E,\mu) = R(E)$, completely ignoring the denominator, $\{\Sigma t(E,z) + \Sigma_0\}$.
- 4) **Unshielded Multi-Group** (defined from 2 Band Parameters, including unresolved) – this should be statistically equivalent to 3), but for this paper starts from 2 band parameters, and combines them to define unshielded cross sections.
- 5) **Totally Shielded Multi-Group** (defined from 2 Band Parameters, including unresolved) – this ignores the presence of any other materials in the mixture,
 $\Phi(E,\mu) = R(E,\mu) / \{\Sigma t(E,z)\}$, assuming $\langle \Sigma_0 \rangle = 0$
- 6) **Partially Shielded Multi-Group** (defined from 2 Band Parameters), including unresolved) – uses the Bondarenko approximation, that each isotope in a material is independent,
 $\Phi(E,\mu) = R(E,\mu) / \{\Sigma t(E,z) + \langle \Sigma_0 \rangle\}$

Here I will note, that this last “definition” is not necessarily unique, because a variety of multi-group processing codes treat $\langle \Sigma_0 \rangle$ differently, e.g., is $\langle \Sigma_0 \rangle$ the shielded or unshielded cross section for all other materials, and is it specific to each material included in each application? Accounting for the actual self-shielding in all other materials would require a multi-group processing code to iterate starting from any “application independent” multi-group data library. Here I use the unshielded cross section for each evaluation, in each group, to define $\langle \Sigma_0 \rangle$ in all cases.

Definition of Criticality

Based on the literature you will find a number of different definitions of k_{eff} ,

- 1) A definition as the **eigenvalue of a mathematical problem**, to find the multiplier of fission ν -bar that will make a system self-sustaining. This can lead to a dangerously low estimate of k_{eff} , if there are any other processes, besides fission, that can contribute neutrons. For example (n,2n) cannot by itself make a system critical, because there is no “upscatter”. However, in the presence of fission, (n,2n) can contribute neutrons to an otherwise sub-critical system and make it critical.
- 2) A definition based on the **balance between neutron production and removal**; where removal includes both neutron absorption and leakage. Unlike definition 1), which only considers fission, this definition includes all neutron production, such as due to (n,2n), etc. For example, with a sub-critical assembly we can add a beryllium reflector, whose high (n,2n) can make the system critical. This is the definition used by the TART Monte Carlo code [3], and of the values presented in this paper.
- 3) A definition based on **Analog** Monte Carlo; for example, tracking neutrons collision by collision, and sampling one, and only one, outcome for each event (collision), only at the spatial point of the collision. This is a rather slowly converging process.
- 4) A definition based on **Expected** Monte Carlo; for example, rather than the Analog method, that only tallies one outcome per event, with Expected we tally continuously along the neutron track, based on ALL the cross sections that contribute to the total cross section. Compared to Analog, this converges more rapidly, particularly for integral parameters, such as k_{eff} . But in some cases, this can lead to loss of important correlations.

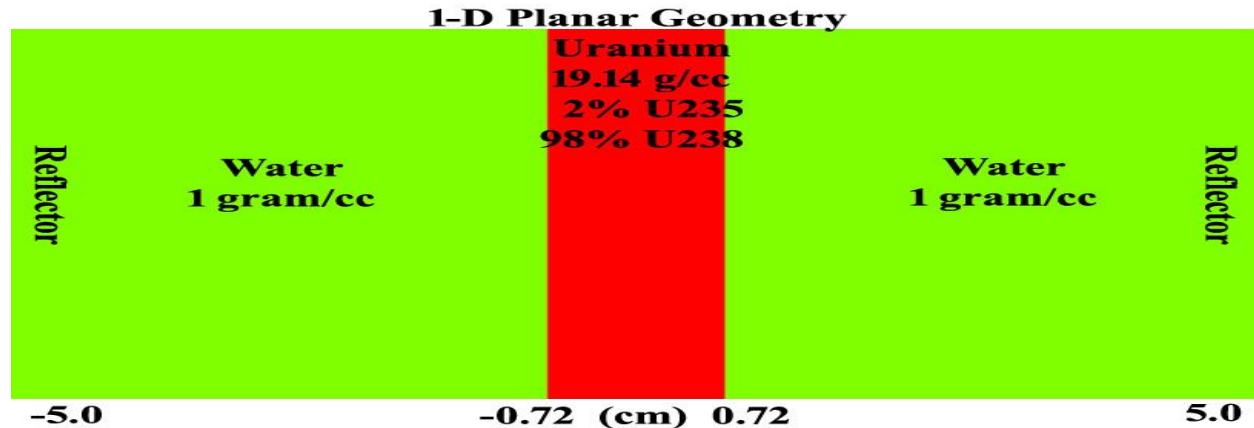
TART [3] tallies both Analog and Expected results. This approach allows comparison of the two “answers” to check for convergence; in an unbiased sample we expect the two to converge to the same answer, as we sample progressively more neutrons. Generally, I quote Expected values in this paper, but I have also included some Analog results, which I have tried to clearly mark.

There are many well documented “critical” systems, for example TART [3] is distributed with over 1,000 “critical” systems [9], which are intended for testing purposes. But we must use caution, and carefully read the documentation for these systems, because not all are for actual critical systems (some are sub-critical), and all are simplified models (geometrically, and often materially). In addition, there is uncertainty in k_{eff} due to the nuclear data used; **the answer of any computer code cannot be any more accurate than the data it uses**. In this paper I assume the BEST, most physically acceptable, answer, will be that based on using the most detailed nuclear data, i.e., Continuous energy cross sections. **WARNING:** Due to the combination of many limitations, for any “approximate” model, the k_{eff} closest to unity, may not be the most “accurate”; again, a reminder that here I assume the answer based on using Continuous energy cross sections is the BEST, and I compare all other to this.

These limitations need not concern us in this paper, because rather than investigating how accurately we can produce k_{eff} , we will only be concerned with **how much k_{eff} is changed due to using one cross section model versus another; particularly, how resonance self-shielding affects k_{eff}** .

Simple, 1-D, Planar Example

To illustrate results I first calculated a very geometrically simple, theoretical critical system of a 1-D, planar, infinitely repeating array of Uranium layers in Water. I start with this extremely simple system to make it as easy as possible for anyone to replicate these results using other neutron transport codes, particularly deterministic codes.



I used continuous energy cross sections as well as the TART 616 groups (50 per energy decade from 10^{-5} eV to 20 MeV) to represent the multi-group and multi-band cross sections (2 bands per group). The only difference in the calculations was the representation of the neutron cross sections as either continuous or multi-group (histograms), e.g., in all six cases I used the same continuous energy neutrons, geometry and reaction kinematics; only the multi-group (histogram), cross sections differed. Today we seem to have FAITH (faith = belief, without proof) that we can calculate k_{eff} to an accuracy of roughly 0.1% (3 digits), whereas the below results illustrate that if we do not account for self-shielding the difference between the results using continuous energy cross sections and 616 groups is over 0.025, 2.5%, or over 25 TIMES what we consider acceptable – let me repeat what I wrote: **the difference is not 25%; it is 25 TIMES the 0.001 in k_{eff} , 0.1%, we consider acceptable. This difference is solely because of our “guess” for the flux that I used to define the multi-group constants, i.e., solely due to the self-shielding model.**

Note the running times: These are typical, showing that today using continuous energy cross sections is no longer prohibitively expensive, which is why **this is “The Standard BEST Option” that I use for all of my TART production work**; here I use multi-group and multi-band results solely in the hope that the results can be useful by others in their multi-group calculations; particularly deterministic calculations.

Planar U/Water Criticality Results

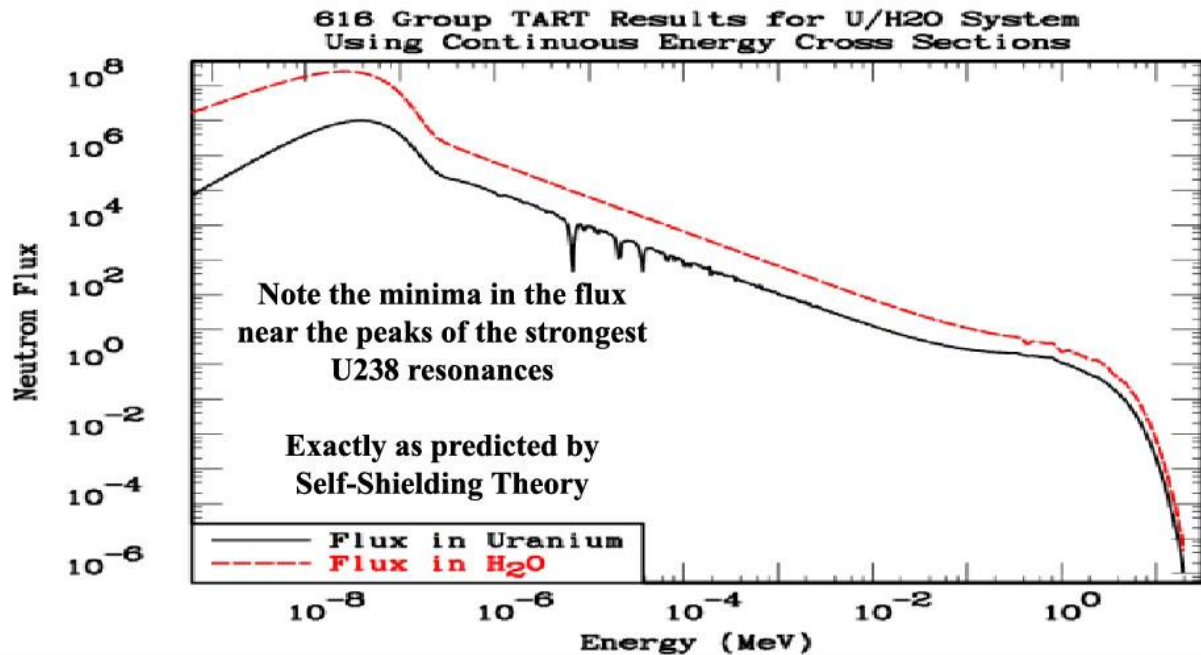
| Cross Section Representation | Expected K-eff | Difference in K-eff | Removal Lifetime (Microsec.) | Median Energy (eV) | Seconds |
|------------------------------|----------------|---------------------|------------------------------|--------------------|----------|
| Continuous | 0.999924 | ----- | 7.89162D+01 | 5.00948D-02 | 5066.660 |
| Multi-Group | 0.974683 | -0.025241 | 7.70376D+01 | 5.01225D-02 | 3837.700 |
| Multi-Band | 1.000980 | 0.001056 | 7.90684D+01 | 5.01097D-02 | 4404.120 |
| Unshielded | 0.974645 | -0.025279 | 7.70372D+01 | 5.01247D-02 | 4442.640 |
| Totally Shielded | 1.001750 | 0.001826 | 7.97356D+01 | 4.95769D-02 | 4581.800 |
| Partial Shielded | 0.991570 | -0.008354 | 7.86170D+01 | 4.98773D-02 | 4512.280 |

Today we have FAITH (again, belief, without proof) that we can calculate critical systems within roughly 0.1%, i.e., 3-digits of accuracy. But the above results using 616 groups, demonstrates that,

- 1) Not self-shielding at all leads to differences of ~ 2.5%; **25 TIMES what we assume.**
- 2) Totally or Partially shielding improves results, but not to ~ 0.1%
- 3) Only the Multi-Band (in this case only 2 Bands) produces agreement ~ 0.1%.

I should stress that this is for a very simple, 1-D planar, system; far from what we expect to find in the real World.

Below is a picture of the neutron flux in the Uranium and Water, separately. The spectrum is more or less what we expect: a fission spectrum at high energy, a 1/E slowing down spectrum at intermediate energies, and a thermal Maxwellian. As it relates to this paper, note the minima in the flux in the Uranium near the peaks of the strongest ²³⁸U resonances; exactly as predicted by Self-Shielding theory. Also, as we expect, there are no such minima in the water; showing the strong spatial dependence of the self-shielding.



PLANE ID: Reaction Details; based on one 10^{+8} neutron sample

The below tables present results using Continuous, Unshielded and Totally Shielded cross sections. Based on these tables it is easy for us to see the sources of the differences in k_{eff} ; I have highlighted the important differences and similarities. Similarities include: All predict about the same ^{238}U fast fission, and (n,2n) contributions (no self-shielding at high energy), as well as that most scatter is in the moderator (H_2O), and no leakage from the system. We see differences in elastic, capture, and fission, i.e., the resonance components.

PLANE ID: Analog Events vs. Isotope per Removed Neutron

Continuous

| Reaction | 92235 | 92238 | 1001 | 8016 |
|----------------|----------------|----------------|-----------------|----------------|
| Elastic | 0.04333 | 1.98132 | 50.68940 | 4.55955 |
| (n,n') | 0.00539 | 0.34429 | 0.00000 | 0.00092 |
| (n,2n) | 0.00002 | 0.00139 | 0.00000 | 0.00000 |
| (n,3n) | 0.00000 | 0.00001 | 0.00000 | 0.00000 |
| Fission | 0.37264 | 0.03073 | 0.00000 | 0.00000 |
| (n,n'p) | 0.00000 | 0.00000 | 0.00000 | 0.00000 |
| (n,n'a) | 0.00000 | 0.00000 | 0.00000 | 0.00001 |
| (n,p) | 0.00000 | 0.00000 | 0.00000 | 0.00001 |
| (n,d) | 0.00000 | 0.00000 | 0.00000 | 0.00000 |
| (n,a) | 0.00000 | 0.00000 | 0.00000 | 0.00242 |
| (n,g) | 0.06893 | 0.15345 | 0.37030 | 0.00011 |
| Totals | 0.49031 | 2.51118 | 51.05970 | 4.56301 |

Unshielded

| Reaction | 92235 | 92238 | 1001 | 8016 |
|----------------|----------------|----------------|-----------------|----------------|
| Elastic | 0.04193 | 2.03861 | 49.64060 | 4.48570 |
| (n,n') | 0.00538 | 0.34454 | 0.00000 | 0.00092 |
| (n,2n) | 0.00002 | 0.00139 | 0.00000 | 0.00000 |
| (n,3n) | 0.00000 | 0.00001 | 0.00000 | 0.00000 |
| Fission | 0.36233 | 0.03078 | 0.00000 | 0.00000 |
| (n,n'p) | 0.00000 | 0.00000 | 0.00000 | 0.00000 |
| (n,n'a) | 0.00000 | 0.00000 | 0.00000 | 0.00001 |
| (n,2a) | 0.00000 | 0.00000 | 0.00000 | 0.00000 |
| (n,p) | 0.00000 | 0.00000 | 0.00000 | 0.00001 |
| (n,d) | 0.00000 | 0.00000 | 0.00000 | 0.00000 |
| (n,a) | 0.00000 | 0.00000 | 0.00000 | 0.00242 |
| (n,g) | 0.06699 | 0.17461 | 0.36134 | 0.00010 |
| Totals | 0.47666 | 2.58994 | 50.00190 | 4.48916 |

Totally Shielded

| Reaction | 92235 | 92238 | 1001 | 8016 |
|----------------|----------------|----------------|-----------------|----------------|
| Elastic | 0.04369 | 1.97345 | 51.12700 | 4.58447 |
| (n,n') | 0.00538 | 0.34430 | 0.00000 | 0.00092 |
| (n,2n) | 0.00002 | 0.00138 | 0.00000 | 0.00000 |
| (n,3n) | 0.00000 | 0.00001 | 0.00000 | 0.00000 |
| Fission | 0.37346 | 0.03075 | 0.00000 | 0.00000 |
| (n,n'p) | 0.00000 | 0.00000 | 0.00000 | 0.00000 |
| (n,n'a) | 0.00000 | 0.00000 | 0.00000 | 0.00001 |
| (n,p) | 0.00000 | 0.00000 | 0.00000 | 0.00001 |
| (n,d) | 0.00000 | 0.00000 | 0.00000 | 0.00000 |
| (n,a) | 0.00000 | 0.00000 | 0.00000 | 0.00243 |
| (n,g) | 0.06705 | 0.15091 | 0.37387 | 0.00011 |
| Totals | 0.48960 | 2.50081 | 51.50090 | 4.58795 |

PLANE ID: Analog Removal and Production per Removed Neutron.

The above table of results are **Expected**, and the below table are **Analog**; note the agreement in all cases to well within 3 digits (yet another indicator of convergence).

| | Expected | Analog |
|------------------|----------|----------|
| Continuous | 0.999924 | 0.999780 |
| Unshielded | 0.974645 | 0.974810 |
| Totally Shielded | 1.001750 | 1.001805 |

Continuous

| Reaction | Removal | Production | Events |
|----------|----------|------------|-----------|
| Elastic | 0.000000 | 0.000000 | 57.273600 |
| (n,n') | 0.000000 | 0.000000 | 0.350596 |
| (n,2n) | 0.001412 | 0.002824 | 0.001412 |
| (n,3n) | 0.000008 | 0.000023 | 0.000008 |
| Fission | 0.403369 | 0.996932 | 0.403369 |
| (n,n'p) | 0.000000 | 0.000000 | 0.000000 |
| (n,n'a) | 0.000000 | 0.000000 | 0.000008 |
| (n,p) | 0.000007 | 0.000000 | 0.000007 |
| (n,d) | 0.000001 | 0.000000 | 0.000001 |
| (n,a) | 0.002419 | 0.000000 | 0.002419 |
| (n,g) | 0.592785 | 0.000000 | 0.592785 |
| Leakage | 0.000000 | 0.000000 | 0.000000 |
| Totals | 1.000000 | 0.999780 | 58.624200 |
| K-eff | | 0.999779 | |

Unshielded

| Reaction | Removal | Production | Events |
|----------|----------|------------|-----------|
| Elastic | 0.000000 | 0.000000 | 56.206800 |
| (n,n') | 0.000000 | 0.000000 | 0.350841 |
| (n,2n) | 0.001410 | 0.002820 | 0.001410 |
| (n,3n) | 0.000008 | 0.000024 | 0.000008 |
| Fission | 0.393117 | 0.971966 | 0.393117 |
| (n,n'p) | 0.000000 | 0.000000 | 0.000000 |
| (n,n'a) | 0.000000 | 0.000000 | 0.000007 |
| (n,2a) | 0.000000 | 0.000000 | 0.000000 |
| (n,p) | 0.000007 | 0.000000 | 0.000007 |
| (n,d) | 0.000001 | 0.000000 | 0.000001 |
| (n,a) | 0.002419 | 0.000000 | 0.002419 |
| (n,g) | 0.603039 | 0.000000 | 0.603039 |
| Leakage | 0.000000 | 0.000000 | 0.000000 |
| Totals | 1.000000 | 0.974810 | 57.557700 |
| K-eff | | 0.974810 | |

Totally Shielded

| Reaction | Removal | Production | Events |
|----------|----------|------------|-----------|
| Elastic | 0.000000 | 0.000000 | 57.728600 |
| (n,n') | 0.000000 | 0.000000 | 0.350606 |
| (n,2n) | 0.001402 | 0.002804 | 0.001402 |
| (n,3n) | 0.000008 | 0.000024 | 0.000008 |
| Fission | 0.404212 | 0.999007 | 0.404212 |
| (n,n'p) | 0.000000 | 0.000000 | 0.000000 |
| (n,n'a) | 0.000000 | 0.000000 | 0.000007 |
| (n,p) | 0.000007 | 0.000000 | 0.000007 |
| (n,d) | 0.000001 | 0.000000 | 0.000001 |
| (n,a) | 0.002434 | 0.000000 | 0.002434 |
| (n,g) | 0.591937 | 0.000000 | 0.591937 |
| Leakage | 0.000000 | 0.000000 | 0.000000 |
| Totals | 1.000000 | 1.001805 | 59.079200 |
| K-eff | | 1.001805 | |

To better understand the source of these differences let's look inside the Uranium to see what's happening as far as the spatially dependent flux and the all-important reaction rates.

Flux, Reactions and Average Total Cross Section vs. Depth into Uranium

Our Monte Carlo codes track neutrons collision by collision; as do discrete ordinate codes when they run analogue sweep by sweep. Let's look inside the Uranium to see the details of what happens for the first collision versus depth into the Uranium. We will be interested in the spatially dependent flux, reaction rates, and "local" average cross section. I will use the Russian ABBN 26 group structure, which allows us to very clearly "see" self-shielding effects; these results will be similar to those seen using any group structure.

PLEASE understand that these are not Monte Carlo results; **they are analytical results** based on using a series of PREPRO [7] codes. The only uncertainty is that of the ENDF/B data [2]; there are no statistical uncertainties, as would occur with Monte Carlo or modelling errors as occur in either Monte Carlo or deterministic codes. Starting from ENDF/B cross section [8] the following series of PREPRO codes were used,

LINEAR/RECENT/SIGMA1: Linearly interpolable, tabulated, 293.6 Kelvin cross sections.

MIXER: Create the Uranium mixture: 2% ²³⁵U, 98% ²³⁸U.

GROUPIE: Calculate ABBN multi-group and multi-band cross sections.

VIRGIN: Calculate uncollided (i.e., virgin) flux, reaction rates, and cross sections.

With this approach the uncollided results are based on the actual Uranium mixture, of 2% ²³⁵U and 98% ²³⁸U, so that we avoid even the "partial" or Bondarenko approximation, i.e., for the multi-group results we need only consider **Unshielded** or **Totally Shielded** results. Anyone can re-create these, or any other, analytical uncollided results by FREELY downloading the ENDF data [8], and my PREPRO codes from my website [7].

The ABBN group structure uses three (3) groups per neutron energy decades; in any decade there are boundaries at 1, 2.15, 4.65, and 10 . Here I will show results only for one energy group from 100 to 215 eV (results in other groups are similar). To allow simple comparisons I will normalize the integral of the incident flux to be unity,

| | Energy Dependent | Group Averaged |
|---------------|--|--|
| Flux | $\text{Exp}[-\Sigma t(E) * z / \mu]$ | $\int_{E_g}^{E_{g+1}} \text{Exp}[-\Sigma t(E) * z / \mu] dE$ |
| Reactions | $\Sigma t(E) * \text{Exp}[-\Sigma t(E) * z / \mu]$ | $\int_{E_g}^{E_{g+1}} \Sigma t(E) * \text{Exp}[-\Sigma t(E) * z / \mu] dE$ |
| Cross Section | Reactions/Flux = $\Sigma t(E)$ | Reactions/Flux = Variable in space |

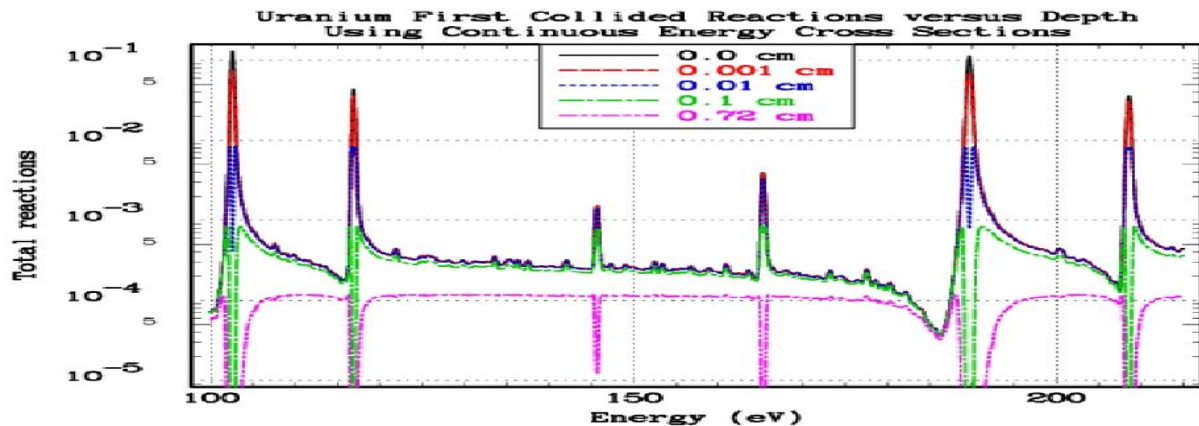
The above results are general, since they apply to using either continuous energy or multi-group cross sections. It is informative to look at the special case where we are using multi-group cross sections, and the energy range that we use corresponds to only one group. Rather than a general energy dependent cross section we have, $\Sigma t(E) = \langle \Sigma t \rangle$; the above general equations reduce to,

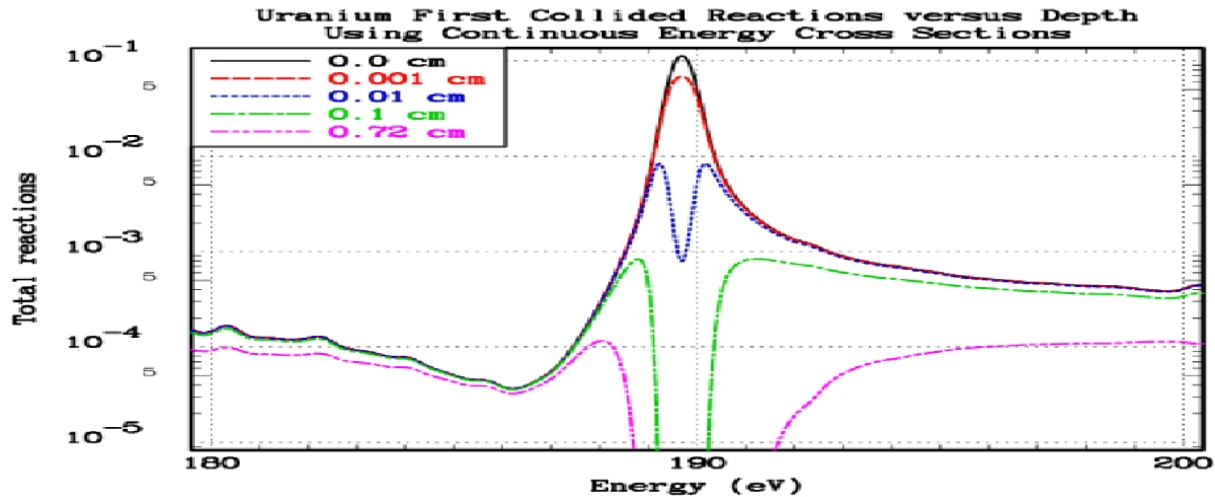
| | Energy Dependent | Group Averaged |
|---------------|--|--|
| Flux | $\text{Exp}[-\langle\Sigma t\rangle * z / \mu]$ | $\text{Exp}[-\langle\Sigma t\rangle * z / \mu]$ |
| Reactions | $\langle\Sigma t\rangle * \text{Exp}[-\langle\Sigma t\rangle * z / \mu]$ | $\langle\Sigma t\rangle * \text{Exp}[-\langle\Sigma t\rangle * z / \mu]$ |
| Cross Section | Reactions/Flux = $\langle\Sigma t\rangle = \mathbf{Constant}$ | Reactions/Flux = $\langle\Sigma t\rangle = \mathbf{Constant}$ |

First let's look at the actual energy dependent first collided total reaction rate versus depth into the Uranium, from a depth 0 to 0.72 cm (the midpoint of the Uranium, in the above simple problem), for the energy range 100 to 215 eV (one of the ABBN groups). This is followed by a detail of the 180 to 200 eV range, to more clearly see the results in one large resonance.

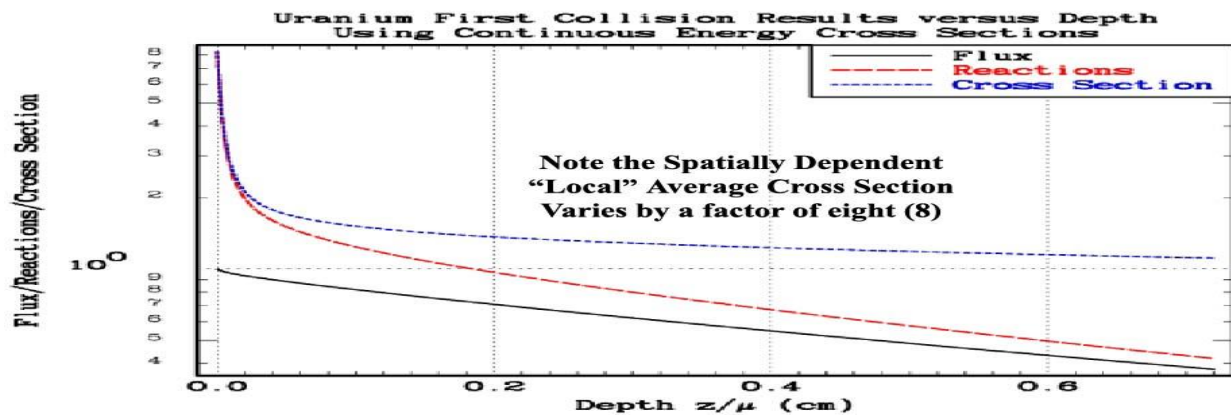
Note the reaction (Y axis) scale. By a depth of 0.72 cm there are virtually no remaining uncollided neutrons near the resonances and compared to the incident reaction rates at the surface (0 cm) the remaining reaction rates are up to 1,000 times lower, basically the only remaining reactions occur in the minima between resonances. From these figures even for very small depth (0.001 cm) we see significant self-shielding; even for as little as 0.0001 cm thickness the analytical calculations show significant reduction in the reaction rate (~ 20%).

What is important for the reader to understand is that in this case there is no reason for us to show the approximate energy dependent reaction used by the ABBN group structure, because by definition of “multi-group”, it is constant across this entire energy range. After “seeing” the actual energy dependent reaction rate in the below figures you might question how accurate multi-group methods can be if they ignore this energy dependence. Multi-group results can be quite accurate, particularly to define simple integral parameters such as k_{eff} .

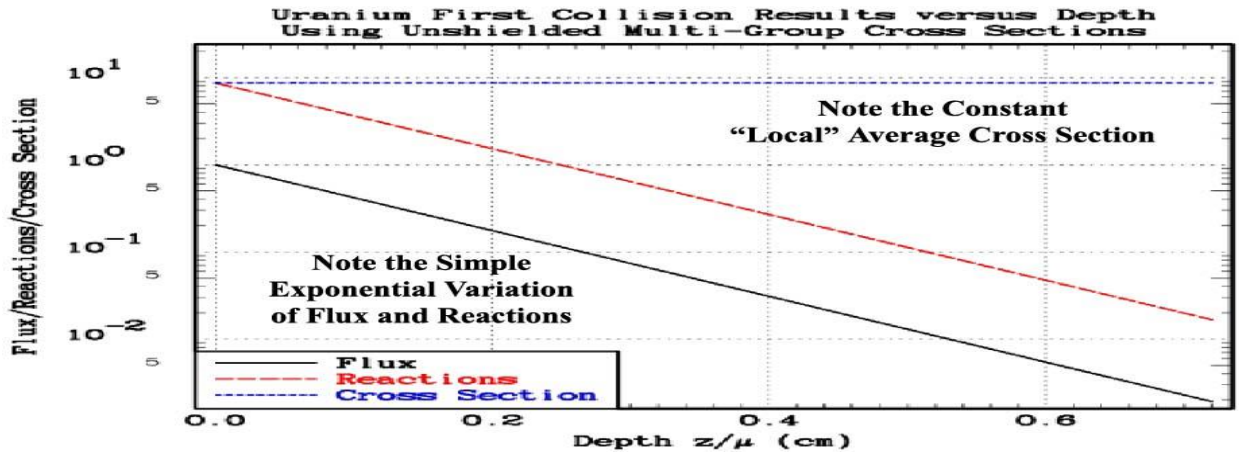




Next let's look at the group integrated results versus depth into the Uranium for the same single ABBN group from 100 to 215 eV. **Using continuous energy cross sections**, at the surface of the Uranium the neutrons have not yet "seen" the Uranium resonances, so strictly by cause and effect, we know there cannot be any self-shielding, i.e., **the correct "local" group averaged cross section MUST be the unshielded value**. As the neutrons progress further into the Uranium neutrons encounter the resonances, and within a very short distance the **energy dependent flux nearest the resonances** is heavily **depressed** (as we have seen in the above energy dependent figures), causing the "local" **group averaged cross section (the ratio of group reactions to flux)** to be dramatically **self-shielded** (as we have seen in the below spatially dependent figures). In the below figure we can see that the "local" group averaged average cross section decreases by about a factor of eight (8), from its highest, unshielded, value at the surface, to its heavily self-shielded value deep within the Uranium – **I repeat: a factor of 8!!!!** Whereas all of our multi-group models assumes it is constant, independent of space within each zone; therein lies the problem with our multi-group models; they all suffer the loss of detail in space and direction.

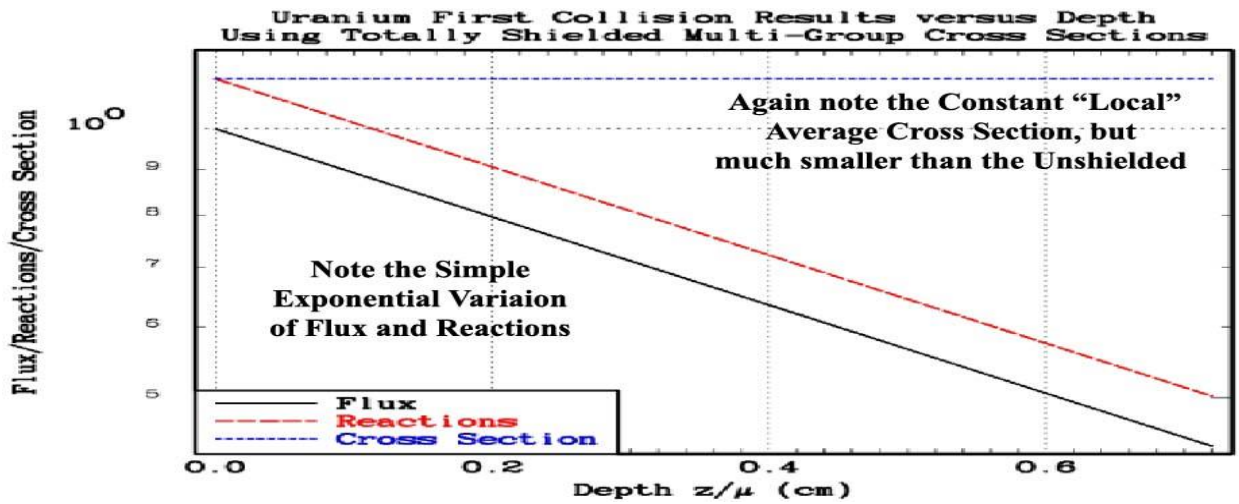


In contrast using **multi-group cross sections**, by definition, for each group the “local” average cross section is independent of depth, which means the flux and reaction rates within each group will show simple exponential attenuation into the Uranium. Using **Continuous Energy** or **Unshielded cross sections**, at the surface the “average” cross section is the same unshielded value, so the reaction rates are the same. However, with **Continuous** energy cross section the “local” cross section decreases with depth, allowing neutrons to penetrate further into the Uranium, making the reaction rate deep within the Uranium much higher than with unshielded multi-group cross sections; **in this case over a factor of more than a hundred (100) times higher.**

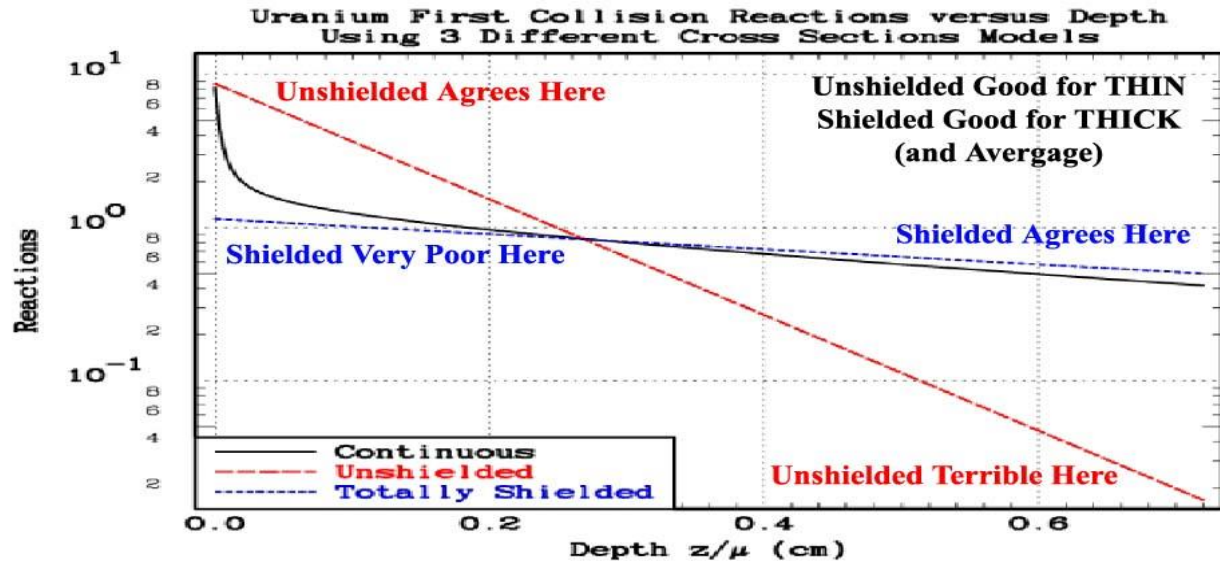


In the above figures the most obvious differences are because using continuous energy cross sections the “local” (z/μ dependent) total cross section is variable, whereas with multi-group cross sections, by definition, the total cross section in any one group is a constant.

Next let’s look at the same results using **Totally self-shielded** cross sections. Here the group averaged cross section is only about 1/8 that of the unshielded cross sections, so that the Uranium is optically thin and there is little attenuation. **Comparing these three figures, particularly the spatially dependent “local” average cross section using Continuous cross sections, to me it is amazing that the calculated k_{eff} only differ by a few per-cent.**

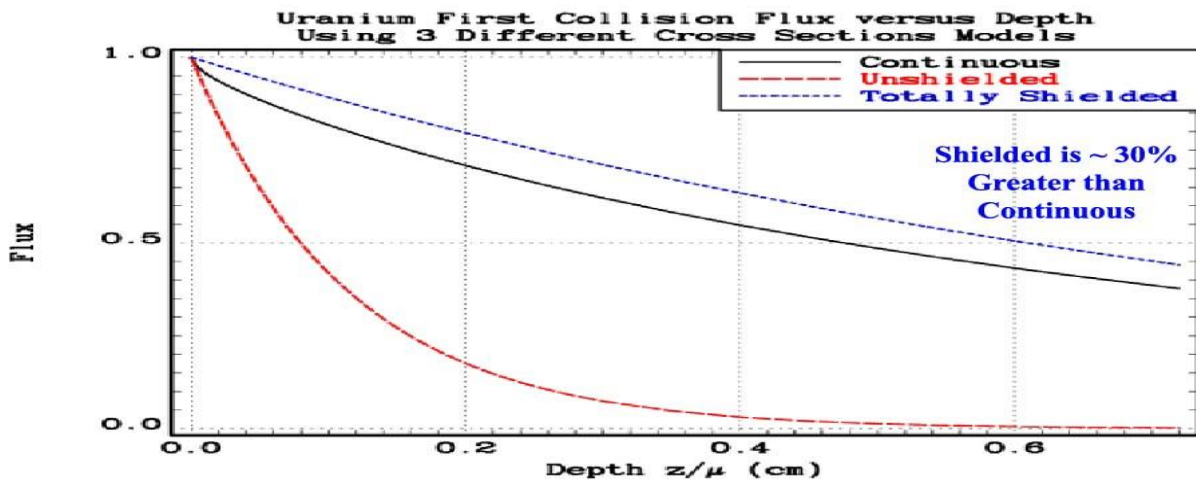
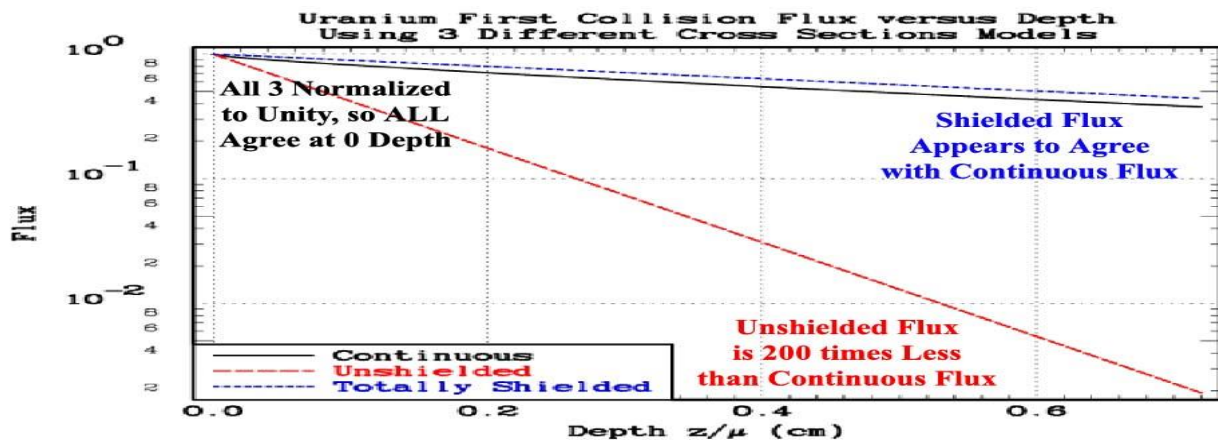


Below when we compare the **total reaction rates vs. depth** for these three cross sections models, we can see that the **Unshielded** model yields the same reaction rate at the surface but varies enormously everywhere else. Whereas **Totally shielding** yields much lower reaction rates near the surface (~ 8 times lower), but pretty good agreement deeper into the Uranium



Through Thick or Thin: The above figure demonstrates that in order to **reproduce the spatially dependent Total Reactions** we need **Unshielded** group averages for **THIN**, or small, depths (or thicknesses), and **Shielded** group averages for **THICK**, or larger, depths (or thicknesses), and to reproduce spatial averages. **With only one degree of freedom (the group average) normal multi-group models cannot simultaneously satisfy both extremes.**

Below plotting the **Flux vs. Depth** clearly shows the problem with **Unshielded** cross sections, where it looks nothing like the **Continuous** cross section results; the Unshielded being up to **200 TIMES less** than the Continuous results. The first below figure seems to show agreement between the **Continuous** and **Totally Shielded** results, however this is only because of the log Y scale. Switching to a linear Y scale, shows that in fact the **Totally Shielded** results are up to 30% greater than the **Continuous** results, and greater than the Continuous at all depths, so its integral will also be greater.



The above simple infinite repeat lattice is by far not the most difficult problem we will face; in general, $k_{\text{eff}} = \text{Production} / [\text{Absorption} + \text{Leakage}]$, but our infinite system has no leakage, so that in this case k_{eff} is merely a ratio of reaction rates. Also, generally we will be interested in more than simple integral parameters, such as k_{eff} . For example, we may also be interested in the **spatially dependent burn-up**, which based on the above plots of **Continuous** reactions, will be high near the surface, as predicted by **Unshielded**, and nothing like the much lower reactions based on **Shielded** cross sections (~ 8 times too low).

Based of the above results, I will summarize the multi-group results by pointing out that in our neutron calculations in general we are interested in the scalar flux and current as well as reaction rate. The problem is that with only one degree of freedom (the multi-group cross sections), we cannot accurately simultaneously satisfy all these needs. Also as mentioned earlier, dividing into finer zones may not help, because using one of these multi-group self-shielding models, all zones may still have the same shielded cross sections.

The Multi-Band method [10, 11,12, 13, 14, 15], is designed to directly address these needs by introducing more degrees of freedom for each of the multi-groups. Physically we can think of each **energy group** divided into N **Total Cross Section Ranges** (Lebesgue integration over cross section, instead of Riemann integration over energy). After our calculation we can add the N results together to define the results for each group . Generally, using N cross section bands per group we have 2*N degrees of freedom; only 2*N – 1, because by definition of sum of the band weights MUST be unity. Here I will only use two (2) cross section bands, so we have four (4) constants that we can define for each group: P1, P2, Σ_{T1} , Σ_{T2} . With this 2-band model the equivalent definitions of flux, reactions and “local” group averaged cross sections become,

| | Group Averaged |
|---------------|---|
| Flux | $P1 * \text{Exp}[-\Sigma_{T1} * z / \mu] + P2 * \text{Exp}[-\Sigma_{T2} * z / \mu]$ |
| Reactions | $\Sigma_{T1} * P1 * \text{Exp}[-\Sigma_{T1} * z / \mu] + \Sigma_{T2} * P2 * \text{Exp}[-\Sigma_{T2} * z / \mu]$ |
| Cross Section | Reactions/Flux = Variable |

Note, here we have two cross sections attenuating the neutrons, compared to only one for the multi-group model. I define these constants to ensure that in certain limiting cases we reproduce the known, or at least expected, limiting values, **basically the THIN and THICK limits** mentioned above,

- 1) $P1 + P2 = 1$ = normalization
- 2) The Unshielded value
- 3) The Totally Shielded value
- 4) One Partially shielded value, to follow expected $\Sigma_0 = 0$ to infinity self-shielding curve

These are four equations in four unknowns, so we expect a unique analytical solution to define four constants: P1, P2, Σ_{T1} , and Σ_{T2} . By inserting three weighting functions into our equation and equating the resulting equations to our **known, three pre-calculated self-shielded cross sections** [7, 16], $\langle \Sigma_0 \rangle$, $\langle \Sigma_1 \rangle$, $\langle \Sigma_2 \rangle$ (Unshielded, Total, Partial),

$$\begin{aligned}
1 &= P_1 + P_2 \\
\langle \Sigma_0 \rangle &= \frac{\Sigma_{T1}P_1 + \Sigma_{T2}P_2}{P_1 + P_2} ; (W(\Sigma_T) = 1) \\
\langle \Sigma_1 \rangle &= \frac{P_1 + P_2}{P_1X_{T1} + P_2X_{T2}} ; (W(\Sigma_T) = X_T) : X_T = 1/\Sigma_T \\
\langle \Sigma_2 \rangle &= \frac{P_1\Sigma_{T1}X_{T1}^* + P_2\Sigma_{T2}X_{T2}^*}{P_1X_{T1}^* + P_2X_{T2}^*} : (W(\Sigma_T) = X_T^*) : X_T^* = 1/[\Sigma_T + \langle \Sigma_0 \rangle]
\end{aligned}$$

These are a set of non-linear equations; in this case with 2 bands, quadratic equations. We all know how to solve a quadratic equation [$x^2 + 2*b*x + c = 0$]; the solution is $A \pm B$, where: $A = -b$, and $B = \text{Sqrt}[b^2 - c]$; it's that simple. I used this to analytically define a unique solution to these four equations. We also know that there are similar solutions to cubic and quartic equations, so I also have analytical solutions for the 3 and 4 band equations, but in almost all cases 2 bands are more than adequate.

Making the standard change of variables used to solve a quadratic equation,

$$P_1 = \frac{1}{2} + \delta ; \Sigma_{T1} = \frac{1}{X_1} = \frac{1}{A+B} ; P_2 = \frac{1}{2} - \delta ; \Sigma_{T2} = \frac{1}{X_2} = \frac{1}{A-B}$$

This change of variables immediately satisfies $P_1 + P_2 = 1$ and the remaining three equations can be analytically solved to define,

$$A = \frac{1}{2 \langle \Sigma_1 \rangle} \left[\frac{\langle \Sigma_0 \rangle - \langle \Sigma_1 \rangle}{\langle \Sigma_0 \rangle - \langle \Sigma_2 \rangle} \right]$$

$$B^2 = \{ \langle \Sigma_1 \rangle A [\langle \Sigma_0 \rangle A - 2] + 1 \} / [\langle \Sigma_0 \rangle \langle \Sigma_1 \rangle]$$

$$\delta = \frac{1 - A \langle \Sigma_1 \rangle}{2B \langle \Sigma_1 \rangle}$$

As expected, there are two possible values for B , corresponding to the positive and negative roots of B^2 . This is the result of the non-uniqueness of the solution without an ordering. From the definitions of Σ_{T1} , Σ_{T2} and δ in terms of A and B , we can see that choosing the positive or negative root of B^2 merely corresponds to the same solution with the two bands interchanged. In order to obtain a unique solution, we will always define B to be positive, which corresponds to introducing the ordering $\Sigma_{T1} \leq \Sigma_{T2}$.

The above algorithm will always produce physically acceptable parameters (positive band weights and cross sections) as long as $\langle \Sigma_0 \rangle \geq \langle \Sigma_2 \rangle \geq \langle \Sigma_1 \rangle$ (Unshielded \geq Partial \geq Total). The only time that the three of these are equal is when the total cross section is independent of energy across the group (i.e., when it is constant); in all other cases this inequality is true. When the cross section is constant the two bands become indistinguishable and the two band cross sections become equal,

i.e., only one band is required in the group (i.e., the normal multigroup equation). WARNING – this is a limiting case that the codes GROUPIE [7], URRDO [5] and URRFIT [6], explicitly handle to avoid a singularity in the above definitions, as B and δ approach zero; this limit and how I handle it is described below.

In the seemingly trivial limit of no self-shielding, these equations become numerically unstable, because in this limit and two band cross sections, Σ_{T1} and Σ_{T2} , approach the unshielded average, and the two band weights, P_1 and P_2 , become non-unique, as long as they sum to unity, e.g., we can see this from the equations defining B and δ , since in the no shielding limit B approaches zero and since δ is proportional to $1/B$, we have a problem.

To handle this limit, I consider three cases. In all three cases I always define,

$$P_1 = \frac{1}{2} + \delta \quad ; \quad \Sigma_{T1} = \frac{1}{X_1} = \frac{1}{A+B} \quad ; \quad P_2 = \frac{1}{2} - \delta \quad ; \quad \Sigma_{T2} = \frac{1}{X_2} = \frac{1}{A-B}$$

The three cases correspond to placing limits on δ and/or B .

- 1) **No self-shielding:** $\langle \Sigma_1 \rangle = \langle \Sigma_0 \rangle$

| | |
|----------|----------------------------|
| Weight | $W(\Sigma_T) = 1$ |
| Conserve | $\langle \Sigma_0 \rangle$ |

$$P1 = P2 = 1/2 : \delta = 0, B^2 = 0, A = 1/\langle \Sigma_0 \rangle$$

$$\Sigma_{T1} = \Sigma_{T2} = \langle \Sigma_0 \rangle$$

- 2) **Little self-shielding:** $\langle \Sigma_1 \rangle \Rightarrow 0.9999 \langle \Sigma_0 \rangle$; 0.01% or less self-shielding

| | | |
|----------|----------------------------|----------------------------|
| Weight | $W(\Sigma_T) = 1$ | $W(\Sigma_T) = 1/\Sigma_T$ |
| Conserve | $\langle \Sigma_0 \rangle$ | $\langle \Sigma_1 \rangle$ |

$$P1 = P2 = 1/2 : \delta = 0$$

$$A = 1/\langle \Sigma_1 \rangle$$

$$B^2 = A^2 [\langle \Sigma_0 \rangle - \langle \Sigma_1 \rangle] / [\langle \Sigma_0 \rangle]$$

3) **General self-shielding:** $\langle \Sigma_1 \rangle < 0.9999 \langle \Sigma_0 \rangle$; more than 0.01% self-shielding

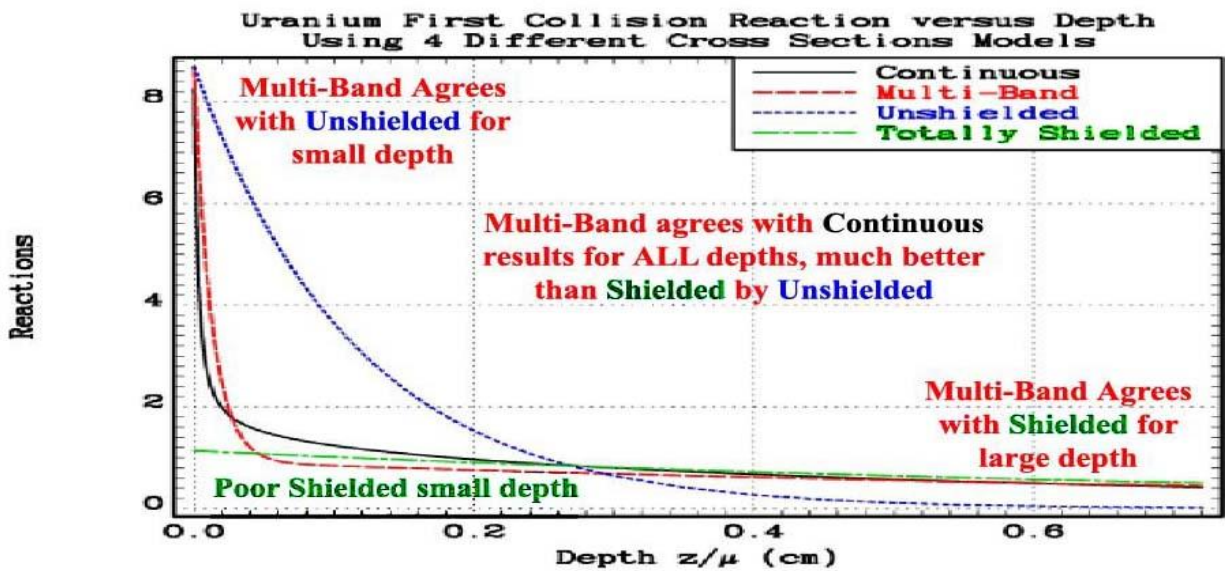
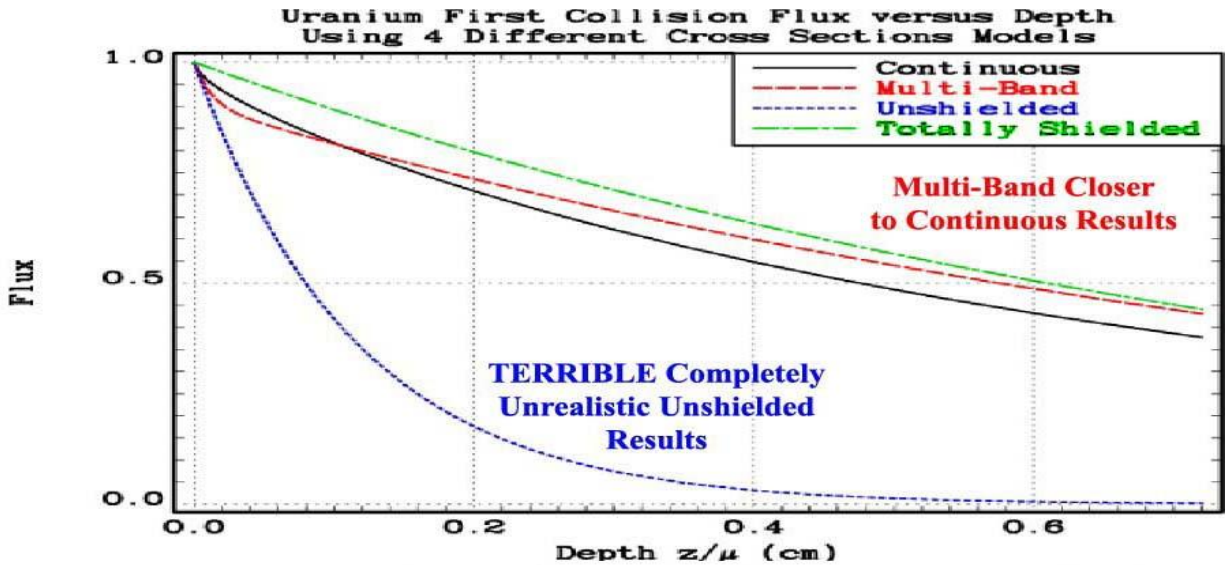
| Weight | $W(\Sigma_T) = 1$ | $W(\Sigma_T) = 1/\Sigma_T$ | $W(\Sigma_T) = 1/(\Sigma_T + \langle \Sigma_0 \rangle)$ |
|----------|----------------------------|----------------------------|---|
| Conserve | $\langle \Sigma_0 \rangle$ | $\langle \Sigma_1 \rangle$ | $\langle \Sigma_2 \rangle$ |

$$A = \frac{1}{2 \langle \Sigma_1 \rangle} \left[\frac{\langle \Sigma_0 \rangle - \langle \Sigma_1 \rangle}{\langle \Sigma_0 \rangle - \langle \Sigma_2 \rangle} \right]$$

$$B^2 = \{ \langle \Sigma_1 \rangle A [\langle \Sigma_0 \rangle A - 2] + 1 \} / [\langle \Sigma_0 \rangle \langle \Sigma_1 \rangle]$$

$$\delta = \frac{1 - A \langle \Sigma_1 \rangle}{2B \langle \Sigma_1 \rangle}$$

Let's look at some results. The first plot below compares **FLUX**; here the **multi-band** results are similar, but somewhat better than the **shielded** results. Where we see the BIG difference is in the second plot below of **TOTAL REACTIONS**; here the multi-band results clearly outperform the shielded and unshielded results. The **multi-band** method reproduces the expected **unshielded** results at the surface (depth = 0), where the **shielded** results are far too low (in this case a factor of ~ 8 too low). The **multi-band** method also reproduces the expected **shielded** results at large depths, where the **unshielded** results are very poor. And most important, across the entire depth range **the multi-band results are in closer agreement with the real Continuous results versus depth, so its integral will be closer, which is what we are interested in to accurately calculate k_{eff} .**



Usually when one thinks of multi-group data, one only considers an “average” over energy, but in fact **the “average” is really over (energy, space, direction)**. Hopefully the above results clearly show the need for improved spatial results, which the multi-band method is designed to provide. Less obvious is that the **multi-band method also improves directional results**. For example, at the surface of the fuel the multi-band method is designed to reproduce the **unshielded incident** flux and reaction rate (as shown above). But it will also reproduce the **shielded leakage** from the surface of the fuel. In other words: **at exactly the same spatial point (the surface) the multi-band method can reproduce the angular incident and reflected flux and reaction rates**; something multi-group “averages” cannot do. This is equivalent in a discrete ordinate code having different “average” cross sections in each discrete direction, which the 2 multi-band cross sections combine to reproduce.

Transmission Measurements

The above results for the Uncollided flux and Reaction Rates are more than an Academic Exercise that we can never actually observe. They correspond to the measurement of well columnated transmission through a range of thicknesses for any given material; in the above case the transmission through a material composed of 2% ^{235}U and 98% ^{238}U . In these measurements, “**self-indication**” corresponds to measuring **reaction rates** and “**flux**” obviously corresponds to the **flux** shown above.

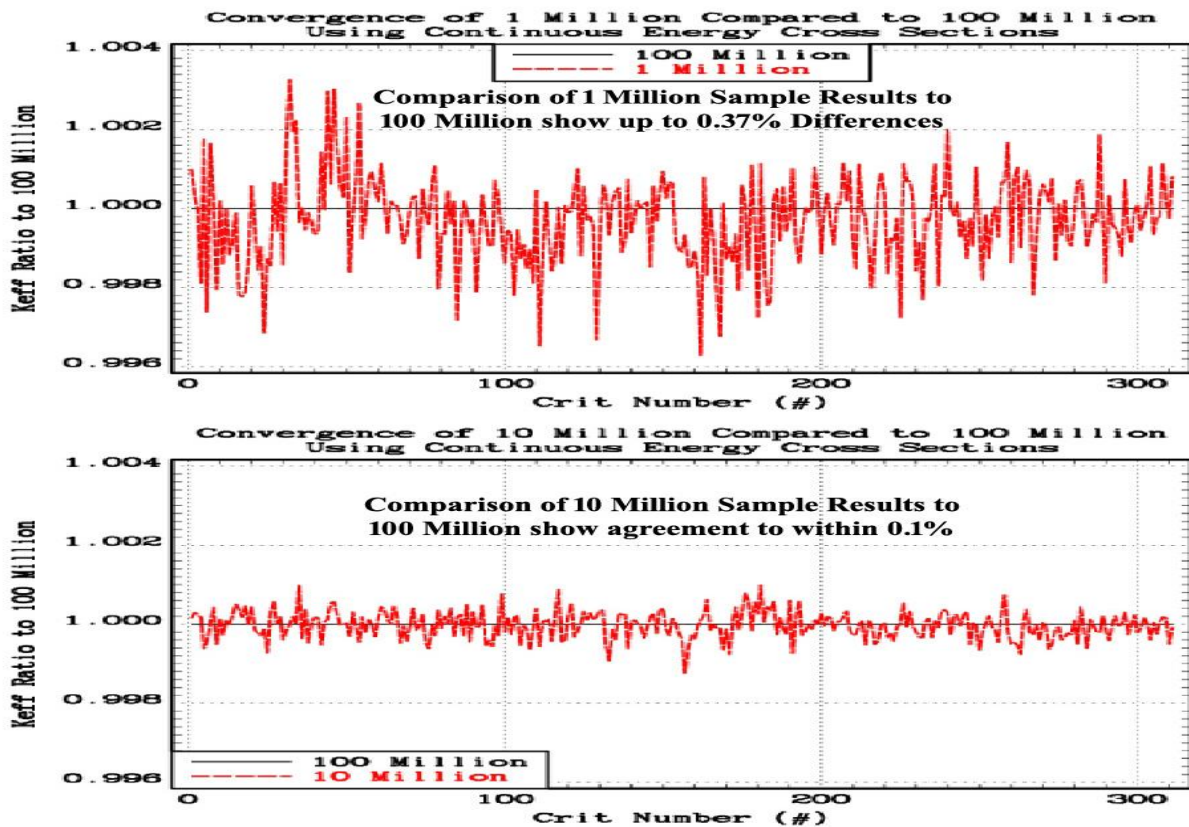
There are many such measurements and reports analyzing these measurements. As it relates to this paper, I will mention the measurements of Bramblett and Czirr for ^{239}Pu [17] and ^{235}U [18], who reported results for transmission measurements through ^{239}Pu and ^{235}U , integrated over a series the ABBN groups, i.e., the same quantities as shown above, but for different materials. These measurements have been extensively analyzed to show the same self-shielding effects [19, 20, 21] as seen in the above figures, so I will not repeat these calculations here. I will merely state that these earlier measurements and calculations verify the self-shielding results shown above, i.e. **these results are real and important to include in multi-group calculations if we expect to produce accurate results, particularly all-important reaction rates.**

It would be wonderful to have a similar self-indication measurement for ^{238}U (hint, for any experimentalists who may be reading this). This would be a very difficult measurement due to the very narrow ^{238}U resonances. The above results indicate that this measurement would require extremely thin foils; the above analytical calculations show that a thickness of only 0.0001 cm (that is not a typo, 10^{-4} cm) reduces the total reaction rate by $\sim 20\%$. By a thickness of only 0.1 cm almost all the self-shielding due to ^{238}U resonance is complete; there are but few neutrons remaining in the energy range of major resonances; see the above plot of the energy dependent spectra versus energy and depth.

Statistics

Unfortunately, too many people assume that since they are using Monte Carlo with continuous energy cross sections this will result in the BEST possible answer. However, anytime we use Monte Carlo we must be sure to run enough samples to insure convergence, this is particularly true when using continuous energy cross sections. When using **multi-group** cross sections our Monte Carlo need only sample a limited number of cross section values. In contrast with **continuous energy cross sections** the code must sample many thousands of tabulated values, as well as the interpolated values between tabulated values. This can require a very large number of samples to TRULY achieve convergence to a final answer.

For the results shown in this report for each of six different cross section models I used 100 million (10^8) neutron samples, for each of 311 ^{235}U slow critical systems [22], i.e., 6 Models X 10^8 samples X 311 assemblies $\sim 2 \cdot 10^{11}$ neutron samples. In my home, on my DELL desktop with 6 processors and 24 GB memory, running all six cross section models simultaneously, this took roughly a week. Was this much time necessary? Yes, if we really want to insure the differences, I present here have truly converged to the accuracy that we claim today. Today many users have FAITH (again, faith = belief, without proof) that we can calculate Monte Carlo criticality k_{eff} results to $\sim 0.1\%$ accuracy (3 digits). Generally, Monte Carlo will converge to one stable final answer with an uncertainty of $R/\text{sqrt}(S)$, where R is a system dependent constant, and S is the number of independent samples used, e.g., **reducing the uncertainty by a factor of 10 requires roughly 100 times as many samples.**



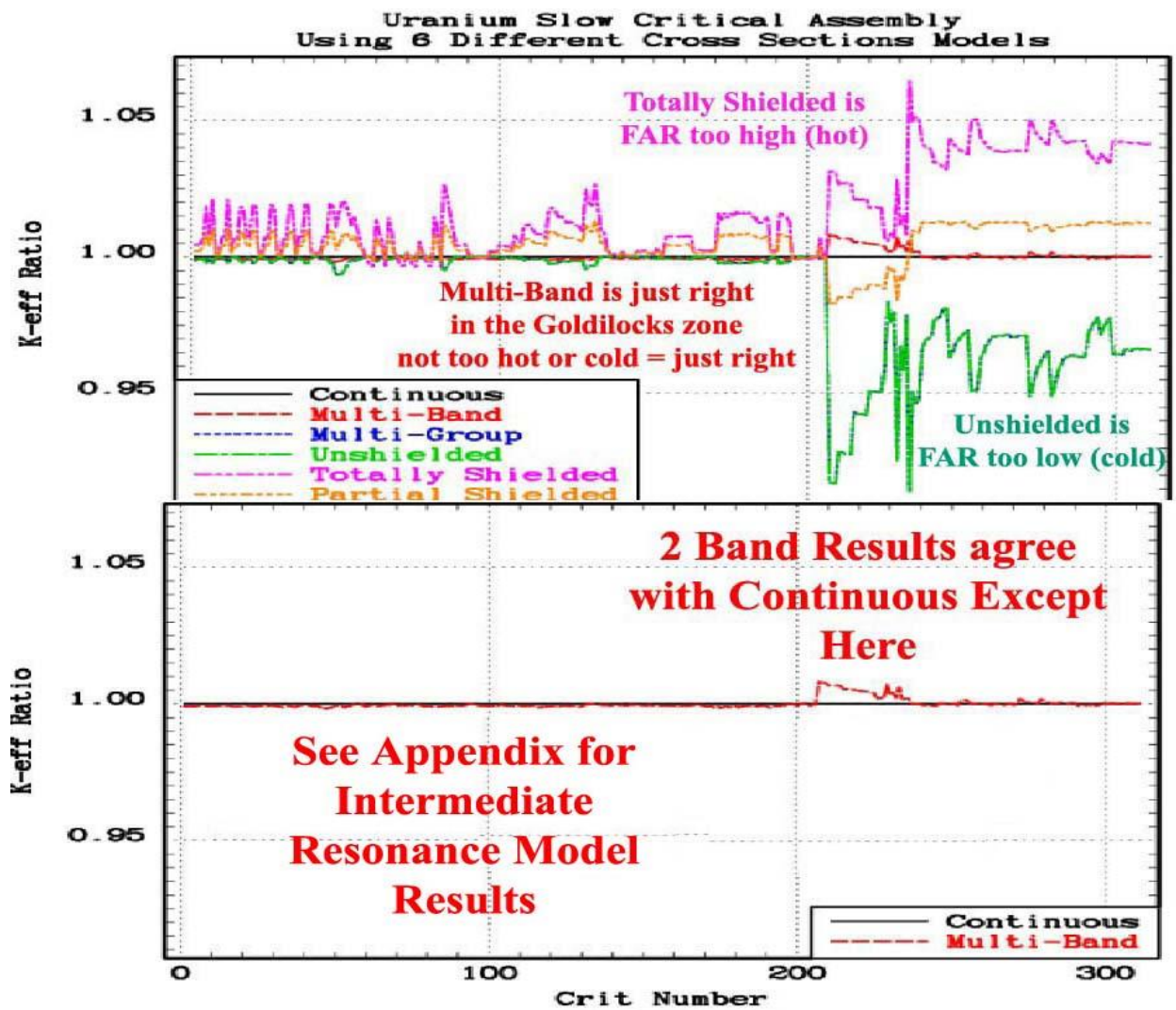
Here to illustrate convergence I used **Continuous** energy cross sections to compare results for 311 ^{235}U slow critical assemblies [8] for: 10^{+6} , 10^{+7} , 10^{+8} , and neutron samples. The above figures show that 10^{+6} results differ from the 10^{+8} results by up to 0.37%, and 10^{+7} results have converged to within 0.1% of the 10^{+8} .

Note the $1/\text{Sqrt}(S)$ convergence: 10^{+6} 0.37%, 10^{+7} 0.1%, and assume (have faith) that the 10^{+8} results are $\sim .03\%$, well within the accuracy we need for this study. Hopefully this explains why I used at least 10^{+8} samples for ALL of the final results = it is necessary to validate the accuracy that I claim.

WARNING: Hopefully these results demonstrate that when comparing differences, as in this study, users must not be in a rush to finish calculations by using too few samples. If you use too few your answers – and conclusions – can be incorrect, and rather than saving time you will end up wasting it.

311 U-235 Slow Critical Assemblies

In an earlier report I published results of k_{eff} calculated by TART [3] for 1,172 Critical Assemblies [22], so this has already been done, and need not be repeated here. Here my focus is not on the BEST calculated k_{eff} , but on rather the difference between the BEST calculated k_{eff} , using **Continuous** energy cross sections, and the five (5) **multi-group** and **multi-band** models discussed here. In order to demonstrate these differences, I used all 311 ^{235}U Slow Assemblies for my earlier report [22]. From the first figure below, we can see that rather than achieving agreement to 0.1% (3 digits), **I found differences up to almost 9% for the multi-group unshielded and shielded models**. In contrast the second figure shows close agreement using 2 Bands, but even it has some problems with assemblies 207 through 231 (LCT006, LMT001, LMT002). In this report I only present 2 bands Narrow Resonance (NR) results, comparable to what other multi-band codes can calculate; see, the appendix for Intermediate Resonance (IR) TART [3] results for assemblies 207 through 231. **Of the models discussed here the multi-band clearly out performs the four strictly multi-group models**.



LCT006-1: Reaction Details; based on one 10^{+8} neutron sample

The below tables present results using Continuous, Unshielded and Totally Shielded cross sections. Based on these tables it is easy for us to see the sources of the differences in K_{eff} ; I have highlighted the important differences and similarities. Similarities include: All predict the same ^{238}U fast fission, and (n,2n) contributions (no self-shielding at high energy), as well as that most scatter is in the moderator (H_2O) (large n,n' is due to bound H) , and small leakage from the system. We see differences in: elastic, capture, and fission, i.e., the resonance components.

LCT006-1: Analog Events vs. Isotope per Removed Neutron

Continuous

| Reaction | 92238 | 92235 | 8016 | 92234 | 13027 | 1001 | 7014 |
|----------------|----------------|----------------|----------------|----------------|----------------|-----------------|----------------|
| Elastic | 1.88951 | 0.05271 | 5.70417 | 0.00064 | 0.38601 | 11.79320 | 0.00017 |
| (n,n') | 0.24331 | 0.00502 | 0.00136 | 0.00002 | 0.01297 | 51.41410 | 0.00000 |
| (n,2n) | 0.00091 | 0.00002 | 0.00000 | 0.00000 | 0.00000 | 0.00000 | 0.00000 |
| (n,3n) | 0.00000 | 0.00000 | 0.00000 | 0.00000 | 0.00000 | 0.00000 | 0.00000 |
| Fission | 0.02204 | 0.38300 | 0.00000 | 0.00003 | 0.00000 | 0.00000 | 0.00000 |
| (n,n'p) | 0.00000 | 0.00000 | 0.00000 | 0.00000 | 0.00002 | 0.00000 | 0.00000 |
| (n,n'a) | 0.00000 | 0.00000 | 0.00001 | 0.00000 | 0.00000 | 0.00000 | 0.00000 |
| (n,p) | 0.00000 | 0.00000 | 0.00001 | 0.00000 | 0.00018 | 0.00000 | 0.00001 |
| (n,d) | 0.00000 | 0.00000 | 0.00000 | 0.00000 | 0.00000 | 0.00000 | 0.00000 |
| (n,t) | 0.00000 | 0.00000 | 0.00000 | 0.00000 | 0.00000 | 0.00000 | 0.00000 |
| (n,a) | 0.00000 | 0.00000 | 0.00386 | 0.00000 | 0.00003 | 0.00000 | 0.00000 |
| (n,g) | 0.18303 | 0.07714 | 0.00010 | 0.00140 | 0.00482 | 0.30584 | 0.00000 |
| Totals | 2.33881 | 0.51789 | 5.70951 | 0.00210 | 0.40403 | 63.51310 | 0.00018 |

Unshielded

| Reaction | 92238 | 92235 | 8016 | 92234 | 13027 | 1001 | 7014 |
|----------------|----------------|----------------|----------------|----------------|----------------|-----------------|----------------|
| Elastic | 1.98423 | 0.04979 | 5.55550 | 0.00059 | 0.37873 | 11.53880 | 0.00016 |
| (n,n') | 0.24260 | 0.00501 | 0.00136 | 0.00002 | 0.01294 | 50.15130 | 0.00000 |
| (n,2n) | 0.00091 | 0.00002 | 0.00000 | 0.00000 | 0.00000 | 0.00000 | 0.00000 |
| (n,3n) | 0.00000 | 0.00000 | 0.00000 | 0.00000 | 0.00000 | 0.00000 | 0.00000 |
| Fission | 0.02201 | 0.34938 | 0.00000 | 0.00003 | 0.00000 | 0.00000 | 0.00000 |
| (n,n'p) | 0.00000 | 0.00000 | 0.00000 | 0.00000 | 0.00002 | 0.00000 | 0.00000 |
| (n,n'a) | 0.00000 | 0.00000 | 0.00001 | 0.00000 | 0.00000 | 0.00000 | 0.00000 |
| (n,p) | 0.00000 | 0.00000 | 0.00001 | 0.00000 | 0.00017 | 0.00000 | 0.00001 |
| (n,d) | 0.00000 | 0.00000 | 0.00000 | 0.00000 | 0.00000 | 0.00000 | 0.00000 |
| (n,t) | 0.00000 | 0.00000 | 0.00000 | 0.00000 | 0.00000 | 0.00000 | 0.00000 |
| (n,a) | 0.00000 | 0.00000 | 0.00386 | 0.00000 | 0.00003 | 0.00000 | 0.00000 |
| (n,g) | 0.23168 | 0.07023 | 0.00009 | 0.00128 | 0.00441 | 0.29873 | 0.00000 |
| Totals | 2.48143 | 0.47443 | 5.56083 | 0.00192 | 0.39631 | 61.98880 | 0.00017 |

Totally Shielded

| Reaction | 92238 | 92235 | 8016 | 92234 | 13027 | 1001 | 7014 |
|----------------|----------------|----------------|----------------|----------------|----------------|-----------------|----------------|
| Elastic | 1.85213 | 0.05411 | 5.79611 | 0.00054 | 0.38256 | 11.93760 | 0.00018 |
| (n,n') | 0.24381 | 0.00505 | 0.00136 | 0.00003 | 0.01300 | 52.39080 | 0.00000 |
| (n,2n) | 0.00092 | 0.00002 | 0.00000 | 0.00000 | 0.00000 | 0.00000 | 0.00000 |
| (n,3n) | 0.00000 | 0.00000 | 0.00000 | 0.00000 | 0.00000 | 0.00000 | 0.00000 |
| Fission | 0.02211 | 0.39577 | 0.00000 | 0.00003 | 0.00000 | 0.00000 | 0.00000 |
| (n,n'p) | 0.00000 | 0.00000 | 0.00000 | 0.00000 | 0.00002 | 0.00000 | 0.00000 |
| (n,n'a) | 0.00000 | 0.00000 | 0.00001 | 0.00000 | 0.00000 | 0.00000 | 0.00000 |
| (n,p) | 0.00000 | 0.00000 | 0.00001 | 0.00000 | 0.00018 | 0.00000 | 0.00001 |
| (n,d) | 0.00000 | 0.00000 | 0.00000 | 0.00000 | 0.00000 | 0.00000 | 0.00000 |
| (n,t) | 0.00000 | 0.00000 | 0.00000 | 0.00000 | 0.00000 | 0.00000 | 0.00000 |
| (n,a) | 0.00000 | 0.00000 | 0.00389 | 0.00000 | 0.00003 | 0.00000 | 0.00000 |
| (n,g) | 0.16668 | 0.07495 | 0.00010 | 0.00102 | 0.00507 | 0.31130 | 0.00000 |
| Totals | 2.28565 | 0.52990 | 5.80148 | 0.00162 | 0.40086 | 64.63970 | 0.00018 |

LCT006-1: Analog Removal and Production per Removed Neutron

Continuous

| Reaction | Removal | Production | Events |
|----------|----------|------------|-----------|
| Elastic | 0.000000 | 0.000000 | 19.826400 |
| (n,n') | 0.000000 | 0.000000 | 51.676700 |
| (n,2n) | 0.000931 | 0.001863 | 0.000931 |
| (n,3n) | 0.000005 | 0.000014 | 0.000005 |
| Fission | 0.405076 | 0.997110 | 0.405076 |
| (n,n'p) | 0.000000 | 0.000000 | 0.000017 |
| (n,n'a) | 0.000000 | 0.000000 | 0.000010 |
| (n,p) | 0.000191 | 0.000000 | 0.000191 |
| (n,d) | 0.000001 | 0.000000 | 0.000001 |
| (n,t) | 0.000000 | 0.000000 | 0.000000 |
| (n,a) | 0.003894 | 0.000000 | 0.003894 |
| (n,g) | 0.572330 | 0.000000 | 0.572330 |
| Leakage | 0.017571 | 0.000000 | 0.000000 |
| Totals | 1.000000 | 0.998987 | 72.485600 |
| K-eff | | 0.998986 | |

Unshielded

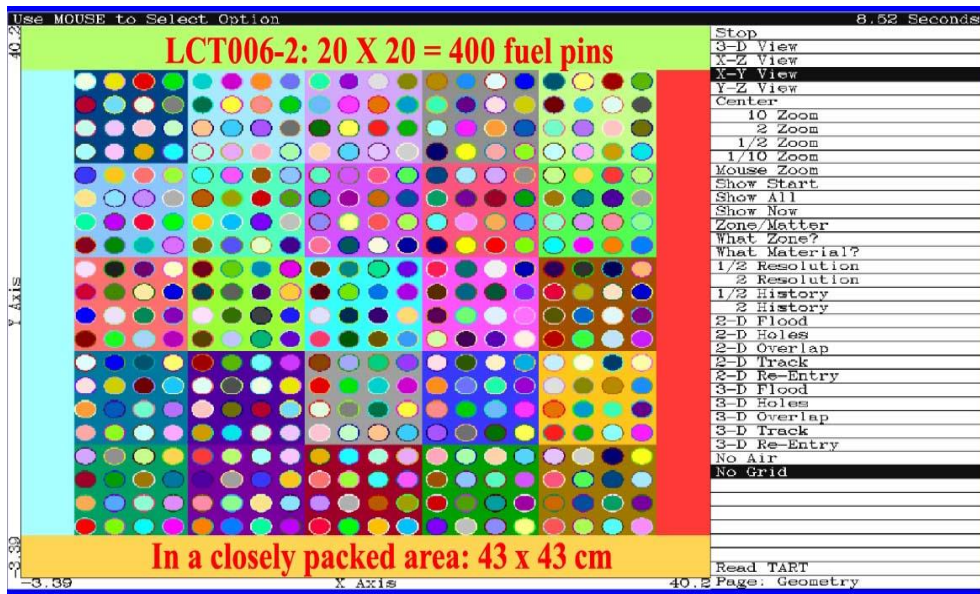
| Reaction | Removal | Production | Events |
|----------|----------|------------|-----------|
| Elastic | 0.000000 | 0.000000 | 19.507800 |
| (n,n') | 0.000000 | 0.000000 | 50.413200 |
| (n,2n) | 0.000933 | 0.001865 | 0.000933 |
| (n,3n) | 0.000005 | 0.000014 | 0.000005 |
| Fission | 0.371423 | 0.915064 | 0.371423 |
| (n,n'p) | 0.000000 | 0.000000 | 0.000018 |
| (n,n'a) | 0.000000 | 0.000000 | 0.000011 |
| (n,p) | 0.000189 | 0.000000 | 0.000189 |
| (n,d) | 0.000002 | 0.000000 | 0.000002 |
| (n,t) | 0.000000 | 0.000000 | 0.000000 |
| (n,a) | 0.003895 | 0.000000 | 0.003895 |
| (n,g) | 0.606421 | 0.000000 | 0.606421 |
| Leakage | 0.017133 | 0.000000 | 0.000000 |
| Totals | 1.000000 | 0.916944 | 70.903900 |
| K-eff | | 0.916943 | |

Totally Shielded

| Reaction | Removal | Production | Events |
|----------|----------|------------|-----------|
| Elastic | 0.000000 | 0.000000 | 20.023300 |
| (n,n') | 0.000000 | 0.000000 | 52.654000 |
| (n,2n) | 0.000938 | 0.001877 | 0.000938 |
| (n,3n) | 0.000005 | 0.000015 | 0.000005 |
| Fission | 0.417913 | 1.028410 | 0.417913 |
| (n,n'p) | 0.000000 | 0.000000 | 0.000018 |
| (n,n'a) | 0.000000 | 0.000000 | 0.000011 |
| (n,p) | 0.000197 | 0.000000 | 0.000197 |
| (n,d) | 0.000001 | 0.000000 | 0.000001 |
| (n,t) | 0.000000 | 0.000000 | 0.000000 |
| (n,a) | 0.003925 | 0.000000 | 0.003925 |
| (n,g) | 0.559116 | 0.000000 | 0.559116 |
| Leakage | 0.017906 | 0.000000 | 0.000000 |
| Totals | 1.000000 | 1.030300 | 73.659400 |
| K-eff | | 1.030300 | |

Is it the model or Statistics?

Before jumping to any conclusions let's take a closer look at these 311 ^{235}U slow critical assemblies. Most of these are geometrically simple large assemblies, that's why we see better agreement for the first 200 or so. But starting with # 207, LCT006-1, there are a series of geometrically complicated assemblies. Below is a TARTCHEK [3] view of LCT006-2 which shows an array of $20 \times 20 = 400$ fuel pins in a roughly 43×43 cm space. Remember, that all four of the Multi-Group models used here assume an **infinite, homogenous** medium (they ignore μK ; directional and spatial streaming). In the LCT006 series there are rather strong neutron currents flowing in and out of each fuel pin, so we would expect differences when we use cross sections designed for infinite, homogeneous models.



Mark Twain said, "There are LIES, DAMN LIES, and STATISTICS". Here I want to be sure we answer the question: **Are the above differences due to the cross section model or statistics?** Even using 10^{+8} active neutrons to calculate each assembly, one might question whether this is sufficient to guarantee convergence, for the LCT006 series, e.g., for each of the 400 fuel pins we are only sampling $10^{+8}/400$ pins = 250,000 neutrons/pin.

In order to test the accuracy of the above results, I re-ran one of the most complicated assemblies, LCT006-1, which is a 19×19 array, similar to the one shown above. I used the TART input option to re-run LCT006-1 100 times, using all six cross section models. To start I ran TART using 1,000 settle cycles (to minimize the effect of the initial flux guess), followed by 10^{+7} active neutrons for each of 100 statistically independent calculations using different random number sequences; this is a cumulative sample of 10^{+9} source neutrons for each of the six cross section models. The below results are absolute k_{eff} results; not ratios to the Continuous results. For each model the below tables define:

- 1) The Average and standard deviation, as well as Lowest and Highest of the 10^{+7} 100 results
- 2) A comparison to a Normal Probability Distribution, as far as the expected distribution of results relative to the average and using the standard deviation.

By 10^{+9} samples the standard deviation of all six models, are well below the 0.1% level. For each model the spread in results and comparison to a Normal Distribution show that even by 10^{+7} , there are no abnormal results beyond +/- 4 standard deviations. **In other words: Statistically this is about as good as it gets. These results demonstrate that the differences are due to the six models, not statistics.**

| | | | | |
|------------------|-----------|---------|-------|--|
| Continuous | 0.9991316 | ----- | ----- | |
| Multi-Group | 0.9169121 | -0.0822 | 8.2% | |
| Unshielded | 0.9169121 | -0.0822 | 8.2% | |
| Multi-Band | 1.0046517 | 0.0055 | 0.5% | |
| Totally Shielded | 1.0302999 | 0.0339 | 3.3% | |
| Partial Shielded | 0.9821768 | -0.0170 | 1.7% | |

The four multi-group models are well in excess 0.1% differences (from 17 up to 82 TIMES). Multi-Band, 2 Band, results differ by 0.5%; extending to 3 Bands eliminates even this difference and achieves our 0.1% goal. I know of no similar improvement I can make to any of the four multi-group models.

| | | | | | | | | | |
|---|----|-----|--------|--------|--|----|-----|--------|--------|
| <u>Continuous</u> Average 0.9991316 +/-0.0002700 Lowest 0.9980110 -0.0011206 Highest 0.9999790 0.0008474 Sample Width Occurrences Per-Cent Per-Cent Range Occurred Normal | | | | | <u>Multi-Band (2 Bands)</u> Average 1.0046517 +/-0.0007666 Lowest 1.0020091 -0.0026446 Highest 1.0067325 0.0020808 Sample Width Occurrences Per-Cent Per-Cent Range Occurred Normal | | | | |
| -4 | -3 | 1 | 1.000 | 0.132 | -3 | -2 | 4 | 4.000 | 2.140 |
| -3 | -2 | 1 | 1.000 | 2.140 | -2 | -1 | 15 | 15.000 | 13.591 |
| -2 | -1 | 13 | 13.000 | 13.591 | 1 | 0 | 31 | 31.000 | 34.134 |
| -1 | 0 | 31 | 31.000 | 34.134 | 0 | 1 | 37 | 37.000 | 34.134 |
| 0 | 1 | 37 | 37.000 | 34.134 | 1 | 2 | 12 | 12.000 | 13.591 |
| 1 | 2 | 13 | 13.000 | 13.591 | 2 | 3 | 2 | 2.000 | 2.140 |
| 2 | 3 | 4 | 4.000 | 2.140 | Sum | | 100 | | |
| Sum | | 100 | | | | | | | |
| <u>Multi-Group</u> Average 0.9169121 +/-0.0002659 Lowest 0.9161100 -0.0008021 Highest 0.9178380 0.0009259 Sample Width Occurrences Per-Cent Per-Cent Range Occurred Normal | | | | | <u>Totally Shielded</u> Average 1.0302999 +/-0.0002789 Lowest 1.0294000 -0.0008999 Highest 1.0311700 0.0008701 Sample Width Occurrences Per-Cent Per-Cent Range Occurred Normal | | | | |
| -3 | -2 | 4 | 4.000 | 2.140 | -3 | -2 | 3 | 3.000 | 2.140 |
| -2 | -1 | 12 | 12.000 | 13.591 | -2 | -1 | 17 | 17.000 | 13.591 |
| -1 | 0 | 34 | 34.000 | 34.134 | -1 | 0 | 26 | 26.000 | 34.134 |
| 0 | 1 | 31 | 31.000 | 34.134 | 0 | 1 | 42 | 42.000 | 34.134 |
| 1 | 2 | 18 | 18.000 | 13.591 | 1 | 2 | 9 | 9.000 | 13.591 |
| 2 | 3 | 1 | 1.000 | 2.140 | 2 | 3 | 3 | 3.000 | 2.140 |
| Sum | | 100 | | | Sum | | 100 | | |
| <u>Unshielded</u> Average 0.9169121 +/-0.0002659 Lowest 0.9161100 -0.0008021 Highest 0.9178380 0.0009259 Sample Width Occurrences Per-Cent Per-Cent Range Occurred Normal | | | | | <u>Partially Shielded</u> Average 0.9821768 +/-0.0002671 Lowest 0.9814710 -0.0007058 Highest 0.983372 0.0011952 Sample Width Occurrences Per-Cent Per-Cent Range Occurred Normal | | | | |
| -3 | -2 | 4 | 4.000 | 2.140 | -3 | -2 | 3 | 3.000 | 2.140 |
| -2 | -1 | 12 | 12.000 | 13.591 | -2 | -1 | 12 | 12.000 | 13.591 |
| -1 | 0 | 34 | 34.000 | 34.134 | -1 | 0 | 31 | 31.000 | 34.134 |
| 0 | 1 | 31 | 31.000 | 34.134 | 0 | 1 | 41 | 41.000 | 34.134 |
| 1 | 2 | 18 | 18.000 | 13.591 | 1 | 2 | 10 | 10.000 | 13.591 |
| 2 | 3 | 1 | 1.000 | 2.140 | 2 | 3 | 2 | 2.000 | 2.140 |
| Sum | | 100 | | | 3 | 4 | 1 | 1.000 | 0.132 |
| | | | | | Sum | | 100 | | |

311 ²³⁵U Slow Critical Assemblies

| | | | | | | | | |
|----|-----------|------|----------|------|-----|-----------|------|----------------|
| 1 | HMT001-1 | U235 | Poly | | 66 | HST006-14 | U235 | Nickel |
| 2 | HMT008-D | U235 | Poly | | 67 | HST006-15 | U235 | Nickel |
| 3 | HMT008-S | U235 | Poly | | 68 | HST006-16 | U235 | Nickel |
| 4 | HST001-1 | U235 | Bare | | 69 | HST006-17 | U235 | Nickel |
| 5 | HST001-2 | U235 | Bare | | 70 | HST006-18 | U235 | Ni-Borated-H2O |
| 6 | HST001-3 | U235 | Bare | | 71 | HST006-19 | U235 | Ni-Borated-H2O |
| 7 | HST001-4 | U235 | Bare | | 72 | HST006-20 | U235 | Ni-Borated-H2O |
| 8 | HST001-5 | U235 | Bare | | 73 | HST006-21 | U235 | Ni-Borated-H2O |
| 9 | HST001-6 | U235 | Bare | | 74 | HST006-22 | U235 | Borated-H2O |
| 10 | HST001-7 | U235 | Bare | | 75 | HST006-23 | U235 | Borated-H2O |
| 11 | HST001-8 | U235 | Bare | | 76 | HST006-24 | U235 | Borated-H2O |
| 12 | HST001-9 | U235 | Bare | | 77 | HST006-25 | U235 | Borated-H2O |
| 13 | HST001-10 | U235 | Bare | | 78 | HST006-26 | U235 | Borated-H2O |
| 14 | HST002-1 | U235 | Steel | case | 79 | HST006-27 | U235 | Nickel& H2O |
| 15 | HST002-2 | U235 | Steel | case | 80 | HST006-28 | U235 | Nickel& H2O |
| 16 | HST002-3 | U235 | Steel | case | 81 | HST006-29 | U235 | Nickel& H2O |
| 17 | HST002-4 | U235 | Steel | case | 82 | HST009-1 | U235 | H2O |
| 18 | HST002-5 | U235 | Al | case | 83 | HST009-2 | U235 | H2O |
| 19 | HST002-6 | U235 | Al | case | 84 | HST009-3 | U235 | H2O |
| 20 | HST002-7 | U235 | Al | case | 85 | HST009-4 | U235 | H2O |
| 21 | HST002-8 | U235 | Al | case | 86 | HST010-1 | U235 | H2O |
| 22 | HST002-9 | U235 | Al | case | 87 | HST010-2 | U235 | H2O |
| 23 | HST002-10 | U235 | Al | case | 88 | HST010-3 | U235 | H2O |
| 24 | HST002-11 | U235 | Al | case | 89 | HST010-4 | U235 | H2O |
| 25 | HST002-12 | U235 | Al | case | 90 | HST011-1 | U235 | Spherical |
| 26 | HST002-13 | U235 | Al | case | 91 | HST011-2 | U235 | Spherical |
| 27 | HST002-14 | U235 | Al | case | 92 | HST012-1 | U235 | H2O |
| 28 | HST003-1 | U235 | Poly | | 93 | HST013-1 | U235 | ORNL-1 |
| 29 | Hst003-2 | U235 | Poly | | 94 | HST013-2 | U235 | ORNL-2 |
| 30 | Hst003-3 | U235 | Poly | | 95 | HST013-3 | U235 | ORNL-3 |
| 31 | Hst003-4 | U235 | Poly | | 96 | HST013-4 | U235 | ORNL-4 |
| 32 | Hst003-5 | U235 | Poly | | 97 | HST014-1 | U235 | H2O |
| 33 | Hst003-6 | U235 | Poly | | 98 | HST014-2 | U235 | H2O |
| 34 | Hst003-7 | U235 | Poly | | 99 | HST014-3 | U235 | H2O |
| 35 | Hst003-8 | U235 | Poly | | 100 | HST015-1 | U235 | H2O |
| 36 | Hst003-9 | U235 | Poly | | 101 | HST015-2 | U235 | H2O |
| 37 | Hst003-10 | U235 | Poly | | 102 | HST015-3 | U235 | H2O |
| 38 | Hst003-11 | U235 | Poly | | 103 | HST015-4 | U235 | H2O |
| 39 | Hst003-12 | U235 | Poly | | 104 | HST015-5 | U235 | H2O |
| 40 | Hst003-13 | U235 | Poly | | 105 | HST016-1 | U235 | H2O |
| 41 | Hst003-14 | U235 | Poly | | 106 | HST016-2 | U235 | H2O |
| 42 | Hst003-15 | U235 | Poly | | 107 | HST016-3 | U235 | H2O |
| 43 | Hst003-16 | U235 | Poly | | 108 | HST017-1 | U235 | H2O |
| 44 | Hst003-17 | U235 | Poly | | 109 | HST017-2 | U235 | H2O |
| 45 | Hst003-18 | U235 | Poly | | 110 | HST017-3 | U235 | H2O |
| 46 | Hst003-19 | U235 | Poly | | 111 | HST017-4 | U235 | H2O |
| 47 | HST004-1 | U235 | 27cm-D2O | | 112 | HST017-5 | U235 | H2O |
| 48 | HST004-2 | U235 | 26cm-D2O | | 113 | HST017-6 | U235 | H2O |
| 49 | HST004-3 | U235 | 25cm-D2O | | 114 | HST017-7 | U235 | H2O |
| 50 | HST004-4 | U235 | 24cm-D2O | | 115 | HST017-8 | U235 | H2O |
| 51 | HST004-5 | U235 | 22cm-D2O | | 116 | HST018-1 | U235 | H2O |
| 52 | HST004-6 | U235 | 30cm-D2O | | 117 | HST018-2 | U235 | H2O |
| 53 | HST006-1 | U235 | Air | | 118 | HST018-3 | U235 | H2O |
| 54 | HST006-2 | U235 | Air | | 119 | HST018-4 | U235 | H2O |
| 55 | HST006-3 | U235 | Air | | 120 | HST018-5 | U235 | H2O |
| 56 | HST006-4 | U235 | Air | | 121 | HST018-6 | U235 | H2O |
| 57 | HST006-5 | U235 | Air | | 122 | HST018-7 | U235 | H2O |
| 58 | HST006-6 | U235 | Air | | 123 | HST018-8 | U235 | H2O |
| 59 | HST006-7 | U235 | Air | | 124 | HST018-9 | U235 | H2O |
| 60 | HST006-8 | U235 | Water | | 125 | HST018-10 | U235 | H2O |
| 61 | HST006-9 | U235 | Water | | 126 | HST018-11 | U235 | H2O |
| 62 | HST006-10 | U235 | Water | | 127 | HST018-12 | U235 | H2O |
| 63 | HST006-11 | U235 | Water | | 128 | HST019-1 | U235 | H2O |
| 64 | HST006-12 | U235 | Nickel | | 129 | HST019-2 | U235 | H2O |
| 65 | HST006-13 | U235 | Nickel | | 130 | HST019-3 | U235 | H2O |

311 ²³⁵U Slow Critical Assemblies (continued)

| | | | | | | | |
|-----|-----------|------|---------|-----|-----------|-------|----------|
| 131 | HST020-1 | U235 | Bare | 196 | HST042-1 | U235 | solution |
| 132 | HST020-2 | U235 | Bare | 197 | HST042-2 | U235 | solution |
| 133 | HST020-3 | U235 | Bare | 198 | HST042-3 | U235 | solution |
| 134 | HST020-4 | U235 | Bare | 199 | HST042-4 | U235 | solution |
| 135 | HST020-5 | U235 | Bare | 200 | HST042-5 | U235 | solution |
| 136 | Hst025-1 | U235 | Water | 201 | HST042-6 | U235 | solution |
| 137 | Hst025-2 | U235 | Water | 202 | HST042-7 | U235 | solution |
| 138 | Hst025-3 | U235 | Water | 203 | HST042-8 | U235 | solution |
| 139 | Hst025-4 | U235 | Water | 204 | HST043-1 | U235 | solution |
| 140 | Hst025-5 | U235 | Water | 205 | HST043-2 | U235 | solution |
| 141 | Hst025-6 | U235 | Water | 206 | HST043-3 | U235 | solution |
| 142 | Hst025-7 | U235 | Water | 207 | LCT006-1 | U235 | Water |
| 143 | Hst025-8 | U235 | Water | 208 | LCT006-2 | U235 | Water |
| 144 | Hst025-9 | U235 | Water | 209 | LCT006-3 | U235 | Water |
| 145 | Hst025-10 | U235 | Water | 210 | LCT006-4 | U235 | Water |
| 146 | Hst025-11 | U235 | Water | 211 | LCT006-5 | U235 | Water |
| 147 | Hst025-12 | U235 | Water | 212 | LCT006-6 | U235 | Water |
| 148 | Hst025-13 | U235 | Water | 213 | LCT006-7 | U235 | Water |
| 149 | Hst025-14 | U235 | Water | 214 | LCT006-8 | U235 | Water |
| 150 | Hst025-15 | U235 | Water | 215 | LCT006-9 | U235 | Water |
| 151 | Hst025-16 | U235 | Water | 216 | LCT006-10 | U235 | Water |
| 152 | Hst025-17 | U235 | Water | 217 | LCT006-11 | U235 | Water |
| 153 | Hst025-18 | U235 | Water | 218 | LCT006-12 | U235 | Water |
| 154 | Hst027-1 | U235 | Bare | 219 | LCT006-13 | U235 | Water |
| 155 | Hst027-2 | U235 | B4C-rod | 220 | LCT006-14 | U235 | Water |
| 156 | Hst027-3 | U235 | B4C-rod | 221 | LCT006-15 | U235 | Water |
| 157 | Hst027-4 | U235 | B4C-rod | 222 | LCT006-16 | U235 | Water |
| 158 | Hst027-5 | U235 | B4C-rod | 223 | LCT006-17 | U235 | Water |
| 159 | Hst027-6 | U235 | Cd-rod | 224 | LCT006-18 | U235 | Water |
| 160 | Hst027-7 | U235 | Cd-rod | 225 | LMT001 | U-nat | D2O |
| 161 | Hst027-8 | U235 | Cd-rod | 226 | LMT002-1 | U235 | D2O |
| 162 | Hst027-9 | U235 | Cd-rod | 227 | LMT002-2 | U235 | D2O |
| 163 | Hst028-1 | U235 | Water | 228 | LMT002-3 | U235 | D2O |
| 164 | Hst028-2 | U235 | Water | 229 | LMT002-6 | U235 | D2O |
| 165 | Hst028-3 | U235 | Water | 230 | LMT002-10 | U235 | D2O |
| 166 | Hst028-4 | U235 | Water | 231 | LMT002-11 | U235 | D2O |
| 167 | Hst028-5 | U235 | Water | 232 | LMT002-12 | U235 | D2O |
| 168 | Hst028-6 | U235 | Water | 233 | LST001 | U235 | Sheba-11 |
| 169 | Hst028-7 | U235 | Water | 234 | LST002-1 | U235 | 15cm-H2O |
| 170 | Hst028-8 | U235 | Water | 235 | LST002-2 | U235 | Bare |
| 171 | Hst028-9 | U235 | Water | 236 | LST002-3 | U235 | 15cm-H2O |
| 172 | Hst028-10 | U235 | Water | 237 | LST003-1 | U235 | Bare |
| 173 | Hst028-11 | U235 | Water | 238 | LST003-2 | U235 | Bare |
| 174 | Hst028-12 | U235 | Water | 239 | LST003-3 | U235 | Bare |
| 175 | Hst028-13 | U235 | Water | 240 | LST003-4 | U235 | Bare |
| 176 | Hst028-14 | U235 | Water | 241 | LST003-5 | U235 | Bare |
| 177 | Hst028-15 | U235 | Water | 242 | LST003-6 | U235 | Bare |
| 178 | Hst028-16 | U235 | Water | 243 | LST003-7 | U235 | Bare |
| 179 | Hst028-17 | U235 | Water | 244 | LST003-8 | U235 | Bare |
| 180 | Hst028-18 | U235 | Water | 245 | LST003-9 | U235 | Bare |
| 181 | Hst029-1 | U235 | Water | 246 | LST004-1 | U235 | 30cm-H2O |
| 182 | Hst029-2 | U235 | Water | 247 | LST004-2 | U235 | 30cm-H2O |
| 183 | HST029-3 | U235 | Water | 248 | LST004-3 | U235 | 30cm-H2O |
| 184 | Hst029-4 | U235 | Water | 249 | LST004-4 | U235 | 30cm-H2O |
| 185 | Hst029-5 | U235 | Water | 250 | LST004-5 | U235 | 30cm-H2O |
| 186 | Hst029-6 | U235 | Water | 251 | LST004-6 | U235 | 30cm-H2O |
| 187 | Hst029-7 | U235 | Water | 252 | LST004-7 | U235 | 30cm-H2O |
| 188 | Hst030-1 | U235 | Water | 253 | LST005-1 | U235 | H2O |
| 189 | Hst030-2 | U235 | Water | 254 | LST005-2 | U235 | H2O |
| 190 | Hst030-3 | U235 | Water | 255 | LST005-3 | U235 | H2O |
| 191 | Hst030-4 | U235 | Water | 256 | LST007-1 | U235 | Bare |
| 192 | Hst030-5 | U235 | Water | 257 | LST007-2 | U235 | Bare |
| 193 | Hst030-6 | U235 | Water | 258 | LST007-3 | U235 | Bare |
| 194 | Hst030-7 | U235 | Water | 259 | LST007-4 | U235 | Bare |
| 195 | HST032-1 | U235 | ORNL-10 | 260 | LST007-5 | U235 | Bare |

311 ²³⁵U Slow Critical Assemblies (continued)

| | | | | | | | |
|-----|----------|------|----------|-----|----------|------|----------|
| 261 | LST009-1 | U235 | Concrete | 287 | LST019-3 | U235 | Poly |
| 262 | LST008-1 | U235 | Concrete | 288 | LST019-4 | U235 | Poly |
| 263 | LST008-2 | U235 | Concrete | 289 | LST019-5 | U235 | Poly |
| 264 | LST008-3 | U235 | Concrete | 290 | LST019-6 | U235 | Poly |
| 265 | LST008-4 | U235 | Concrete | 291 | LST020-1 | U235 | H2O |
| 266 | LST009-2 | U235 | Concrete | 292 | LST020-2 | U235 | H2O |
| 267 | LST009-3 | U235 | Concrete | 293 | LST020-3 | U235 | H2O |
| 268 | LST010-1 | U235 | Poly | 294 | LST020-4 | U235 | H2O |
| 269 | LST010-2 | U235 | Poly | 295 | LST021-1 | U235 | Bare |
| 270 | LST010-3 | U235 | Poly | 296 | LST021-2 | U235 | Bare |
| 271 | LST010-4 | U235 | Poly | 297 | LST021-3 | U235 | Bare |
| 272 | LST016-1 | U235 | 30cm-H2O | 298 | LST021-4 | U235 | Bare |
| 273 | LST016-2 | U235 | 30cm-H2O | 299 | LST022-1 | U235 | case-136 |
| 274 | LST016-3 | U235 | 30cm-H2O | 300 | LST022-2 | U235 | case-135 |
| 275 | LST016-4 | U235 | 30cm-H2O | 301 | LST022-3 | U235 | case-134 |
| 276 | LST016-5 | U235 | 30cm-H2O | 302 | LST022-4 | U235 | case-138 |
| 277 | LST016-6 | U235 | 30cm-H2O | 303 | LST023-1 | U235 | TwoTanks |
| 278 | LST016-7 | U235 | 30cm-H2O | 304 | LST023-2 | U235 | TwoTanks |
| 279 | LST017-1 | U235 | Bare | 305 | LST023-3 | U235 | TwoTanks |
| 280 | LST017-2 | U235 | Bare | 306 | LST023-4 | U235 | TwoTanks |
| 281 | LST017-3 | U235 | Bare | 307 | LST023-5 | U235 | TwoTanks |
| 282 | LST017-4 | U235 | Bare | 308 | LST023-6 | U235 | TwoTanks |
| 283 | LST017-5 | U235 | Bare | 309 | LST023-7 | U235 | TwoTanks |
| 284 | LST017-6 | U235 | Bare | 310 | LST023-8 | U235 | TwoTanks |
| 285 | LST019-1 | U235 | Poly | 311 | LST023-9 | U235 | TwoTanks |
| 286 | LST019-2 | U235 | Poly | | | | |

Boundary Conditions

Physically the correct boundary conditions are simple to state: we require continuity of the neutron flux, using continuous energy, multi-group or multi-band cross sections.

This is EXTREMELY important, because the results in this paper, and other related papers, indicate that the reason the Probability Table Method (PTM) and Multi-Band Method (MB), with all of their apparent approximations, are so successful is not because of what is happening inside the fuel, but rather by improving what's incident and reflected on the surface of the fuel; all this needs is the correct distribution of total cross sections, and is independent of the NR, SLBW, and other limitations of PTM and MB. As shown in the above figures, this is something **Continuous** energy cross sections, and **Multi-Band** cross section can do, for thin and thick systems, but **Multi-Group**, with only one degree of freedom, cannot do.

With **Monte Carlo** codes this is easy for us to accomplish: in TART after each "event" (be it a source, collision, fission, etc.) I sample cross sections for **each isotope** that the neutron encounters. I then use these cross sections until the next "event", regardless of how many different spatial zones the neutron may pass through between "events". For example, in the above simple Uranium/water assembly, if an "event" occurs in the Uranium I separately sample ^{235}U and ^{238}U cross sections, which is all I need to start tracking the neutron. If the neutron leaves the Uranium and enters the water, I sample H and O cross sections, and continue tracking. If the neutron track leaves the water and enters another Uranium zones, I know that I have already sampled the ^{235}U and ^{238}U , so I need not sample any more cross sections to continue tracking the neutron. **This cross section "memory" is imperative to accomplish the correct boundary conditions** (Nikolaev's all the way method [23]); easy to do in a Monte Carlo code. Consider the multi-band method using only 2 bands, I'll refer to these as the smaller and larger totals. If in the first Uranium zone I randomly select the smaller cross section this greatly increases the probability that the neutron will leak from the Uranium, transport through the water, and enter a second Uranium pin. It is then **imperative** that in the second Uranium pin we continue to use the already sampled smaller cross section. This is the only way we can guarantee satisfying the correct boundary conditions, and correctly define the so called Dancoff correction factor for the coupling between surrounding fuel pins. If we mistakenly re-sample the Uranium cross section when entering the second pin, we lose the strong correlation to leakage from the first pin, and overestimate the ^{235}U and ^{238}U cross sections, immediately overestimating the reaction rate from the surface and into the second pin.

With **multi-group** codes continuity of the **multi-group** flux at boundary is easy to accomplish. Unfortunately, continuity of **multi-band** flux is much more difficult. The analogy to the method I described above for Monte Carlo infers 2 bands for each isotope, and per group: with N isotopes we end up with 2^N cross section bands. For the simple U/water example with 4 evaluations, 2^4 , or 16 bands per group; for a problem with 10 isotopes (more realistic), 2^{10} , or 1,204 bands per group (Nikolaev's all the way method [23]). While theoretically correct, for any real problems this quickly becomes impractical in a deterministic code; this is an obvious advantage of Monte Carlo over multi-group. However, multi-group is still so widely used it is worth investigating approximate boundary conditions.

The above results demonstrate accuracy problem with standard multi-group methods, but these results can be improved by focusing on the source of the differences, which is self-shielding in the fuel. For example, much of the difference can be eliminated by using 2 bands in the fuel, to correct self-shielding, and normal multi-group cross sections in the water. For the simple U/water presented here I prepared 2 band cross sections for the Uranium mixture (2% ^{235}U , 98% ^{238}U). This accounts for self-shielding and calculates k_{eff} values very similar to those I calculate with the standard multi-band TART method, described above.

Infinite and Homogeneous

The simple example presented earlier is an **infinite** system, but it is not **infinite** and **homogeneous**, which, by ignoring the spatial and directional effect, μK , is what the multi-group models presented here assume. But obviously the simple example is a heterogeneous system, with separate layers of Uranium and Water; here we expect large spatially currents between the Uranium and Water, as shown in the above plots of flux and reactions. In this case ignoring the spatial and directional effect, μK , would seem to be difficult to justify.

In order to show how heterogeneous effects self-shielding, I homogenized the simple example of Uranium and Water, by mixing the two together, and changing the ^{235}U enrichment to make the resulting homogeneous system close to critical.

| Cross Section Presentation | Infinite | | Infinite & Homogeneous | |
|----------------------------|----------|------------|------------------------|------------|
| | K-eff | Difference | K-eff | Difference |
| Continuous | 0.999924 | ----- | 0.999816 | ----- |
| Multi-Group | 0.974683 | -0.025241 | 0.966235 | -0.033581 |
| Multi-Band | 1.000980 | 0.001056 | 1.000680 | 0.000864 |
| Unshielded | 0.974645 | -0.025279 | 0.966169 | -0.033647 |
| Total Shielded | 1.001750 | 0.001826 | 0.999059 | -0.000757 |
| Partial Shielded | 0.991570 | -0.008354 | 0.986059 | -0.013757 |

The above table shows the heterogenous (identical to the earlier table) and homogeneous results side-by-side. The results to note include,

- 1) Unshielded results in BIG differences: heterogenous 2.52% ; homogeneous 3.35% .
- 2) Partial Shielding yields mixed results: heterogeneous 0.8%; homogenous 1.3%.
- 3) Totally Shielding in heterogeneous within 0.2%; homogeneous is within 0.1%.
- 4) In both cases, Multi-Band is near or within 0.1%.

The bottom line is that,

- 1) Self-shielding is always important; failure to include it results in **differences in k_{eff} over 25 to 22 TIMES the 0.1 we believe we can achieve.**
- 2) Standard multi-group self-shielding improves k_{eff} results close to 0.1; here 0.1 to 0.2.
- 3) Only Multi-band agrees within or close to 0.1.

Beyond these k_{eff} results, I will remind readers of the important spatial and directional effects seen in the above plots; standard multi-group results differ by large factors, whereas multi-band results agree much closer for both thin and thick systems. **This would suggest that if you are interested in spatially dependent effects, such as fuel burnup, normal multi-group is not for you. Whereas, continuous and/or multi-band will need your needs.**

Homogeneous: Analog Events vs. Isotope per Removed Neutron

Continuous

| Reaction | 92235 | 92238 | 1001 | 8016 |
|----------|---------|----------|---------|---------|
| Elastic | 1.36013 | 26.23770 | 0.61951 | 0.12478 |
| (n,n') | 0.16432 | 3.49912 | 0.00000 | 0.00001 |
| (n,2n) | 0.00021 | 0.00432 | 0.00000 | 0.00000 |
| (n,3n) | 0.00000 | 0.00002 | 0.00000 | 0.00000 |
| (n,4n) | 0.00000 | 0.00000 | 0.00000 | 0.00000 |
| Fission | 0.27713 | 0.10661 | 0.00000 | 0.00000 |
| (n,n'a) | 0.00000 | 0.00000 | 0.00000 | 0.00000 |
| (n,p) | 0.00000 | 0.00000 | 0.00000 | 0.00000 |
| (n,a) | 0.00000 | 0.00000 | 0.00000 | 0.00004 |
| (n,g) | 0.06680 | 0.54486 | 0.00001 | 0.00000 |
| Totals | 1.86859 | 30.39260 | 0.61952 | 0.12483 |

Homogeneous: Analog Removal and Production per Removed Neutron

The above table of results are **Expected**, and the below table are **Analog**; note the agreement in all cases to well within 3 digits (yet another indicator of convergence).

Expected 0.999924
 Analog 0.999874

Continuous

| Reaction | Removal | Production | Events |
|----------|----------|------------|-----------|
| Elastic | 0.000000 | 0.000000 | 28.342100 |
| (n,n') | 0.000000 | 0.000000 | 3.663460 |
| (n,2n) | 0.004535 | 0.009070 | 0.004535 |
| (n,3n) | 0.000024 | 0.000072 | 0.000024 |
| (n,4n) | 0.000000 | 0.000000 | 0.000000 |
| Fission | 0.383742 | 0.990734 | 0.383742 |
| (n,n'a) | 0.000000 | 0.000000 | 0.000000 |
| (n,p) | 0.000000 | 0.000000 | 0.000000 |
| (n,a) | 0.000036 | 0.000000 | 0.000036 |
| (n,g) | 0.611665 | 0.000000 | 0.611665 |
| Leakage | 0.000000 | 0.000000 | 0.000000 |
| Totals | 1.000000 | 0.999876 | 33.005600 |
| K-eff | | 0.999874 | |

The Unresolved Resonance Region

Even codes that use continuous energy cross sections, must account for self-shielding in the unresolved resonance region (URR) [1]. In earlier papers [5, 6] we address this point, using NJOY [16] and MCNP [4], with and without self-shielding in the URR. The following test were performed

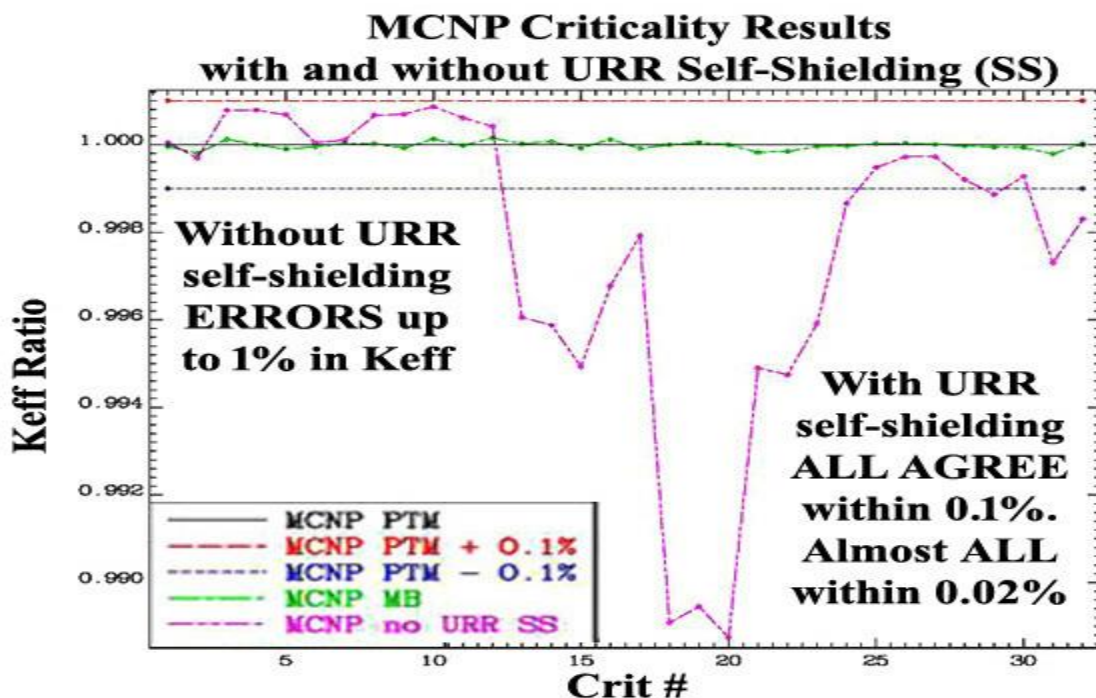
First, we demonstrated the importance of self-shielding in the URR by performing MCNP [4] calculations of 32 critical assemblies with and without URR self-shielding; all these results are based on running an unmodified version of MCNP. The following results are for,

- 1) Not including URR self-shielding (SS), i.e., using unshielded, or infinitely dilute.
- 2) Using the Probability Table Method (PTM), with 20 cross section bands [24, 25].
- 3) Using the Multi-Band Method, using only 2 cross section bands.

On the below figure the MCNP PTM +/- 0.1% lines are included merely as eye guides.

In the below figure the crit # corresponds to the numbers in the critical assembly in following table. Even without identifying the individual assemblies the below figure clearly shows that,

- 1) In these cases, unresolved region self-shielding (URR SS) had an important macroscopic effect on the results. **Here we see that if we do not account for URR SS the answers can be up to 1% different** from the standard MCNP results with URR SS, well outside the accuracy we are attempting to achieve.
- 2) In ALL these cases **the results using 20 PTM bands or 2 MB bands are indistinguishable**, well within 0.1% of one another; indeed, almost ALL are within 0.02% of one another, far below the level of agreement we require in our applications.



32 Critical Assemblies used for MCNP Results

| Crit # | ICSBEP label | Short name | Common name |
|--------|-------------------|------------|-----------------------------------|
| 1 | HEU-MET-FAST-001 | hmf001 | Godiva |
| 2 | HEU-MET-FAST-002 | hmf002-2 | Topsy-2 |
| 3 | HEU-MET-FAST-003 | hmf003-01 | Topsy-U_2.0in(Uranium reflector) |
| 4 | HEU-MET-FAST-003 | hmf003-02 | Topsy-U_3.0in(Uranium reflector) |
| 5 | HEU-MET-FAST-003 | hmf003-03 | Topsy-U_4.0in(Uranium reflector) |
| 6 | HEU-MET-FAST-003 | hmf003-10 | Topsy-W_4.5in(Tungsten reflector) |
| 7 | HEU-MET-FAST-003 | hmf003-11 | Topsy-W_6.5in(Tungsten reflector) |
| 8 | HEU-MET-FAST-014 | hmf014 | VNIIIEF-CTF-DU |
| 9 | HEU-MET-FAST-032 | hmf032-1 | COMET-TU1_3.93in |
| 10 | HEU-MET-FAST-032 | hmf032-2 | COMET-TU1_3.52in |
| 11 | HEU-MET-FAST-032 | hmf032-3 | COMET-TU1_1.742in |
| 12 | HEU-MET-FAST-032 | hmf032-4 | COMET-TU1-0.683in |
| 13 | IEU-MET-FAST-007 | imf007 | Big_Ten |
| 14 | IEU-MET-FAST-007 | imf007d | Big_Ten(detailed) |
| 15 | IEU-MET-FAST-010 | imf010 | ZPR-6/9(U9) |
| 16 | IEU-MET-FAST-013 | imf013 | ZPR-9/1(Tungsten reflector) |
| 17 | IEU-MET-FAST-014 | imf014-2 | ZPR-9/2(Tungsten reflector) |
| 18 | MIX-MISC-FAST-001 | mif001-01 | BFS-35-1 |
| 19 | MIX-MISC-FAST-001 | mif001-02 | BFS-35-2 |
| 20 | MIX-MISC-FAST-001 | mif001-03 | BFS-35-3 |
| 21 | MIX-MISC-FAST-001 | mif001-09 | BFS-31-4 |
| 22 | MIX-MISC-FAST-001 | mif001-10 | BFS-31-5 |
| 23 | MIX-MISC-FAST-001 | mif001-11 | BFS-42 |
| 24 | IEU-MET-FAST-022 | imf022-01 | FR0_3X-S |
| 25 | IEU-MET-FAST-022 | imf022-02 | FR0_5-S |
| 26 | IEU-MET-FAST-022 | imf022-03 | FR0_6A-S |
| 27 | IEU-MET-FAST-022 | imf022-04 | FR0_7-S |
| 28 | IEU-MET-FAST-022 | imf022-05 | FR0_8-S |
| 29 | IEU-MET-FAST-022 | imf022-06 | FR0_9-S |
| 30 | IEU-MET-FAST-022 | imf022-07 | FR0_10-S |
| 31 | IEU-MET-FAST-012 | imf012 | ZPR-3/41 |
| 32 | IEU-COMP-FAST-004 | icf004 | ZPR-3/12 |

The reason the 2 band Multi-Band results produces results equivalent to 20 band PTM results is in the difference between how the bands and weights are defined: Multi-Band explicitly conserves expected limiting values of the total cross section (exactly, without any statistics), while PTM does not explicitly conserve anything (it randomly samples ladders to some statistical level). For more on this topic, see details in refs. [5, 6], and/or the brief summary in the Appendix on PTM vs. MB Methods.

Conclusions

In this paper I describe why Resonance Self-Shielding is so important, and I present examples to illustrate the magnitude of this effect. More importantly, in order to improve the accuracy of our results, I address what can be done to improve our treatment of self-shielding. Throughout I use recent ENDF data [1, 2], and Monte Carlo codes TART [3], and MCNP [4].

I point out the difference between Monte Carlo and deterministic codes (e.g., Sn), as it relates to how each treats self-shielding; particularly regarding boundary conditions. By definition self-shielding means using energy averaged cross sections: obviously this applies to multi-group codes, but it also applies even to codes that use continuous energy cross sections [3, 4], to correctly include self-shielding in the unresolved resonance region [5, 6].

Lastly, I address the question of the statistical accuracy of Monte Carlo codes, and I present numerous examples, both very simple theoretical results, and hundreds of critical assemblies.

Please note that today our computers are fast enough and large enough that for my own applications with my TART Monte Carlo code [3], I always use Continuous energy cross sections, not multi-group. Therefore, self-shielding is no longer a problem I must deal with, except in the unresolved resonance region [5, 6], where an “energy average” statistical approach is still required and used by both TART [3], and MCNP [4], see the appendix for details.

My conclusions include,

- 1) Failure to account for resonance self-shielding can give RUBBISH results. When you use unshielded cross sections be aware: **The results from any computer code can be no better than the data they use**; with unshielded cross sections you can in a: garbage in, garbage out, situation.
- 2) Standard methods of self-shielding in principle only apply to infinite, homogeneous media, but in practice they produce surprisingly accurate results for integral parameters, such as k_{eff} . However, they fail to accurately account for important spatial and directional results simultaneously for thick and thin media, such as spatially dependent fuel burn-up.
- 3) The multi-band method is designed to accurately reproduce both integral parameters, such as k_{eff} , as well as spatial and directional results, for media which are optically thick or thin media (multi-group does not), and generally agrees with results based on using continuous energy cross sections.

The multi-band method as used by TART [3] is used at all energies, whereas with MCNP [4], it has only been applied to self-shielding in the unresolved energy range. The multi-band method owes much to the earlier work of Nikolaev [23] and Levitt [24, 25]; it differs in providing an analytical solution to the multi-band equations, to explicitly conserve expected moments of the flux and reaction rates, and in using Monte Carlo [3], to make practical the correct, all important, boundary conditions, ala Nikolaev’s all the way approach [23]. The results included in this report are based on using the multi-band method in the TART Monte Carlo code [3] for over 40 years, during which time it has been applied to thousands of applications.

Acknowledgment

I thank **Andrej Trkov** (NDS, IEAE, Vienna), for reviewing a preliminary version of this paper and making many helpful suggestions, that have been incorporated into the final version. In also thank **Andrej Trkov** and **Kira Nathani** (NDS, IAEA, Vienna), for editing and producing the final version of this paper as an IAEA report.

References

- [1] “**ENDF-6 Formats Manual** Data Formats and Procedures for the Evaluated Nuclear Data File ENDF/B-VI and ENDF/B-VII”, Written by the Members of the Cross Sections Evaluation Working Group; Last Revision, Edited by M. Herman and A. Trkov, February 2018.
- [2] “**ENDF/B-VII.0: Next Generation Evaluated Nuclear Data Library for Nuclear Science and Technology**”, with M.B. Chadwick and many others, Nucl. Data Sheets **107** (2006), and, “**ENDF/B-VIII.0: The 8th Major Release of the Nuclear Reaction Data Library with CIELO-project Cross Sections, New Standards and Thermal Scattering Data**”, with D.A.Brown and many others, Nucl. Data Sheets **148** (2018).
- [3] “**TART 2016: An Overview of a Coupled Neutron-Photon 3-D, Combinatorial Geometry Time Dependent Monte Carlo Transport Code**”, Report: LLNL-SM-704560, Code Release: LLNL-CODE-708759, September 2016.
- [4] “**MCNP - A General Monte Carlo N-Particle Transport Code**”, Version 5, Vol. I: Overview and Theory, X-5 Monte Carlo Team, Los Alamos National Laboratory report LA-UR-03-1987 (April 24, 2003).
- [5] “**An Alternate Approach to Creating ACE Files for Use in Monte Carlo Codes**”, INDC(NDS)-0701, December 2015, Nuclear Data Section, IAEA, Vienna, Austria. <https://www-nds.iaea.org/publications/indc/indc-nds-0701/>
- [6] “**URR-PACK: Calculating Self-Shielding in the Unresolved Resonance Energy Range**”, INDC(NDS)-0711, Rev. 1, July 2016, Nuclear Data Section, IAEA, Vienna, Austria. <https://www-nds.iaea.org/publications/indc/indc-nds-0711/>
- [7] “**PREPRO2017: 2017 ENDF/B Pre-processing Codes**”, IAEA-NDS-39, Rev. 17, May 2017. (ENDF/B-VII or Proposed VIII Tested); codes are freely available on-line at, <http://redcullen1.net/HOMEEMPAGE.NEW/index.htm>
- [8] “**POINT2018: ENDF/B-VIII Final Temperature Dependent Cross Section Library**”, IAEA-NDS-227, April 2018, Nuclear Data Section (NDS), IAEA, Vienna, Austria. <https://www-nds.iaea.org/publications/nds/iaea-nds-0227/>
- [9] “**ENDF/B-VII.0 Data Testing Using 1,172 Critical Assemblies**”, Lawrence Livermore National Laboratory, UCRL-TR-235178, October 2007
- [10] “Application of the **Probability Table Method** in multi-group calculations”, BNL-50387 (ENDF-187), May 1973.
- [11] "Application of the **Probability Table Method** to Multi-Group Calculations," Nuc. Sci. Eng. **56**, 387-400 (1974).

- [12] "Direct Calculation of **Cross Section Probability Tables**", Trans. Amer. Nucl. Soc. **23**, 526 (1976).
- [13] "Calculation of Probability Table Parameters to Include **Intermediate Resonance Self-Shielding**," Lawrence Livermore Laboratory Report UCRL-79761, San Francisco, CA, December 1977.
- [14] D.E. Cullen, Yigal Ronen (Ed.): "**Nuclear Cross Section Processing**", Handbook of Nuclear Reactor Calculation, vol. I, CRC Press, Inc., Boca Raton, Florida (1986).
- [15] D.E.Cullen, "**Nuclear Data Preparation**", pp. 279-425, Vol. 1, in: "The Handbook of Nuclear Engineering", Springer Publishing, NY, NY (2010).
- [16] R.E. MacFarlane, et al.: The **NJOY** Nuclear Data Processing System, Version 2012, LA-UR-12-27079, August 2013.
- [17] **Pu239**: R.L.Bramblett and J.B.Czirr, "Measurements of Fissions Produced in Bulk Plutonium-239 by 2 eV to 10 keV Neutrons", Nucl. Sci. Eng. **28**, 62-71 (1967).
- [18] **U235**: R.L.Bramblett and J.B.Czirr, "Energy-Dependent Self-Shielding Factors for U235 Foils from Transmission Measurements", Nucl. Sci. Eng. **35**, 350-357 (1969).
- [19] E.F.Plechaty and D.E.Cullen, "Calculation of Resonance Self-Shielding in **U235**", UCID-16359, (1973), Lawrence Livermore National Laboratory.
- [20] E.F.Plechaty and D.E.Cullen, "Calculation of Resonance Self-Shielding in **Pu239**", UCID-16433, (1974), Lawrence Livermore National Laboratory.
- [21] E.F.Plechaty and D.E.Cullen, "Resonance Self-Shielding Calculations Using the **Probability Table Method**", UCID-17230, (1976), Lawrence Livermore National Laboratory.
- [22] with Ernest F. Plechaty, "ENDF/B-VII.0 Data Testing Using **1,172 Critical Assemblies**", Lawrence Livermore National Laboratory, UCRL-TR-235178, October 2007.
- [23] Nikolaev, M.N., and Phillipov, V.V., Atomic Energy **15**, 493 (1963).
- [24] L.B. Levitt: "The probability table method for treating unresolved resonances in Monte Carlo calculations", BNL-50387 (ENDF-187), May 1972.
- [25] L.B. Levitt: "The probability table method for treating unresolved resonances in Monte Carlo calculations", Nucl. Sci. Eng. **49**, No 4, 450-457 (1972).
- [26] Stewart, J.C., J. Quant. Spectrosc. Radiat. Transfer **4**, 723 (1964).
- [27] Goldstein, R., and Cohen, "Theory of Resonance Absorption of Neutrons", Nucl. Sci. Eng. **13**, 132-140 (1962).
- [28] Goldstein, R., "Temperature-Dependent Intermediate Neutron Resonance Integrals", Nucl. Sci. Eng. **48**, 248-254 (1972).
- [29] Goldstein, R., Trans. Am. Nucl. Soc. **21**, 493 (1975).

APPENDICES

A Long History of Time

We have come so far since the beginning of ENDF, over 50 years ago, but I fear that today we are repeating some of the mistakes we made and corrected many years ago. When ENDF started the U.S. nuclear data effort was relatively small and uncoordinated, with each Lab or company independently handling their own nuclear data needs. In this situation at each site all the nuclear needs were met by a relatively small number of people, which had the advantage that it was the same people who selected the basic data, processed it, and then used it in their applications. But the lack of coordination meant that it was difficult to compare results or properly test data, in any attempt to improve the basic data. It was so bad that the two main U.S. nuclear reactor producers could each independently design their type of reactor, but they couldn't design the reactor built by the other company, e.g., their codes and nuclear data were incompatible.

One important step in the ENDF effort was to standardize definitions, and document them in the ENDF Formats and Convention Manual, ENDF-102 [1]. This allowed ENDF users to become more specialized, with experts in different areas concentrating strictly on their own area of expertise and relying on everyone else to follow the strict rules and definitions documents in ENDF-102. As a result, today we have on one side experts on nuclear physics producing ENDF data using their nuclear model codes, and on the other side experts on neutron transport codes using their expertise to use this data in their applications.

There are a number of important steps needed to go from evaluated data in the ENDF format to the form it is used in our transport codes. The two extreme ends of the ENDF chain are manned by experts in nuclear physics and measurements, as well as creating evaluated data and on the other end of the ENDF chain we have experts on neutron transport codes. But what I see as the weak link “**nuclear data processing**” is a less attractive activity, often performed by individuals with little or no background in either creating evaluations or using the data in transport codes. The result can be limitations in the accuracy of our best neutron transport codes because of the processed data they are supplied directly from the nuclear data processing codes.

Here, in this paper, I focused on but one important point: **resonance self-shielding**, and how it can affect the accuracy of our multi-group neutron transport codes. In the hope that it helps, I will merely repeat what I have been saying for decades,

The results of computer codes can be no more accurate than the input data they use.

Or more bluntly: **Garbage in, garbage out.**

A Brief History of Time

In 1972 I first heard Leo Levitt describe his Probability Table Method (PTM), that handles the effect of self-shielding in the **unresolved resonance region** using Monte Carlo calculations [24, 25]. I immediately saw the potential to use Leo's PTM method **over the entire neutron energy range**, using deterministic codes as well as Monte Carlo codes [3, 4]. Only after my first publication did we (Leo Levitt and I) learn of the earlier work in multi-group transport or diffusion, by Nikolaev and Phillipov for neutrons [23], and Stewart for photons [26]; they originated the idea of within each group characterizing the neutrons or photons by the value of the total cross section with which they interact. We must particularly note the work of Nikolaev, who extensively published on this subject, but unfortunately too many of his publications are not available in the West, in English. I am certainly indebted to the work and ideas of Nikolaev, who kindly made me aware of his works.

When I first saw the Levitt's PTM equations [24, 25], I was working on non-linear problems, so I recognized how to analytically solve these equations to define the multi-band weights and cross sections. By 1975 I had implemented what I call the multi-band (MB) method in our TART Monte Carlo code [3] to account for self-shielding across the entire neutron energy range; including the intermediate resonance (IR) method [27, 28, 29], rather than the narrow resonance (NR) used in PTM. This was only possible by using Monte Carlo, to make handling boundary conditions [23] practical, in combination with my analytical parameters.

By now we have over 40 years of experience using the multi-band method in thousands of different neutron calculations. Over those years I have continued to use TART to compare Monte Carlo results using a variety of models, including continuous energy cross sections, versus multi-band to account for self-shielding, versus multi-group with and without for self-shielding. The work that I was doing I documented in textbooks, such as the Handbook of Nuclear reactor Calculations (1986) [14] and more recently the Handbook of Nuclear Engineering (2010) [15]. Also, over the years I have provided computer codes that could be used by others to prepare nuclear data [7] and perform Monte Carlo calculations [3].

When we started work on this self-shielding problem over 40 years ago, computers were too slow and too small to allow us to routinely use continuous energy cross sections, so at the time we heavily relied on the multi-band method. Today's computers are so much faster and bigger that for all my real applications I use continuous energy cross sections, except in the unresolved resonance region, where statistical sampling is still necessary [23, 24, 25]. Even though I personally no longer use the multi-band method across the entire energy range, here I have tried to briefly summarize these 40 years of experience, in the hope that it saves the reader from having to re-invent the wheel and to allow you to more quickly understand the multi-band method: how and why it works and how to use it, particularly in the hope that this method can be used in deterministic codes.

Probability Table versus Multi-Band Methods

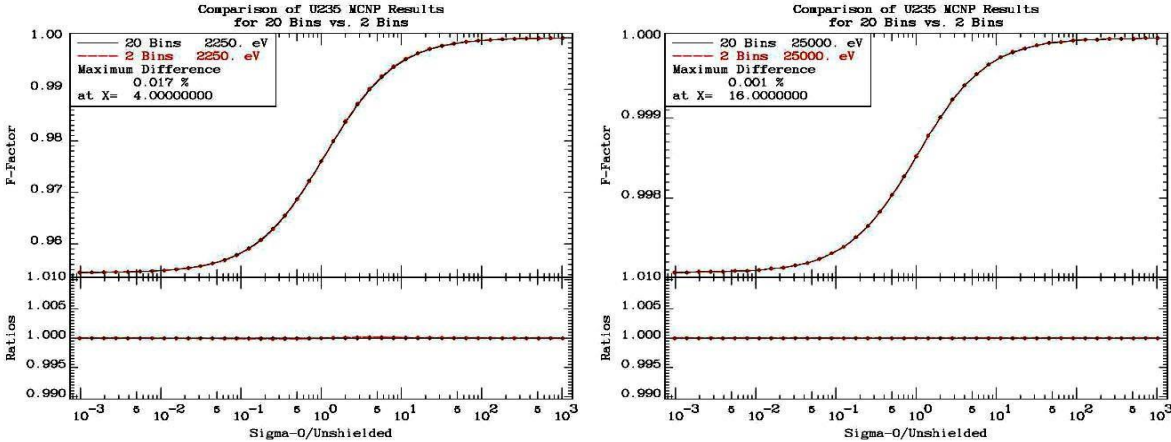
Much of this section have been copied from earlier reports [5, 6]. To better understand the similarities and difference between these two methods, let's look at some real cases, such as ENDF/B-VII.1 ^{235}U and ^{238}U , in the **unresolved resonance region** to see what we are trying to approximate,

| Material | Unresolved Energy Range | Most self-shielding = lowest $f(0)$ factor |
|------------------|-------------------------|--|
| ^{235}U | 2.25 to 25 keV | 0.9544 ~ 4.6% lower than unshielded |
| ^{238}U | 20 to 149 keV | 0.8667 ~ 12.3% lower than unshielded |

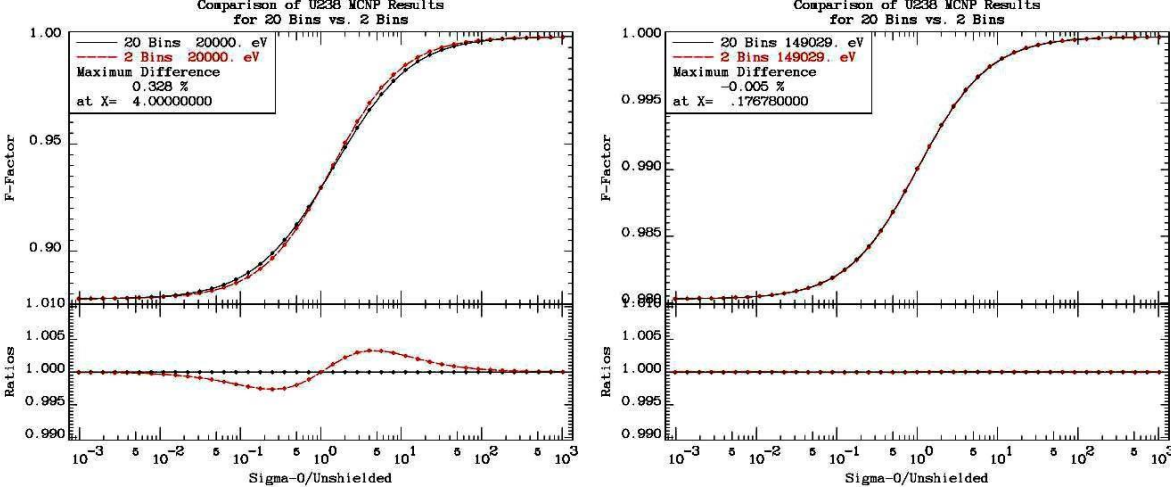
Here we see that the variation of the self-shielded cross section in the unresolved resonance energy range is quite small, e.g., ^{235}U only a maximum of 4.6% change and ^{238}U only a maximum of 12.3%. These differences are certainly large enough to affect macroscopic quantities, such as K_{eff} for critical assemblies, so that self-shielded in the unresolved resonance energy range is important to include in our calculations. But they are relatively easy to accurately represent with a very low order rational, or Pade approximation [14, 15]. **Indeed, our comparison of K_{eff} for a variety of critical assemblies listed above show that these integrals results are statistically indistinguishable whether we use 20 PTM bands or only 2 MB bands.**

How can only 2 multi-band (MB) bands replace 20 probability table method (PTM) bands and still produce accurate results? It is shown that both methods “look” exactly the same (they are both discrete quadratures), and as such **either can be used in ACE [5] files as input to MCNP [4] without making any changes in MCNP; MCNP doesn't know whether it is using PTM or MB data**, e.g., that's why we were able to obtain ALL of the MCNP results presented here without making ANY – repeat ANY – changes to MCNP . Based on the approximations used by the PTM and MB method both are shown to be using a rational, or Pade, approximation, to represent the self-shielded cross section for all values of Σ_0 between zero and infinity. This sounds like a difficult task, but, the variation in the self-shielded cross section in the unresolved energy range is quite small, so that even only 2 MB bands are adequate to reproduce integral results that are indistinguishable from the results obtained using 20 PTM bands.

If we look at the self-shielding curve for Σ_0 between zero and infinity, using 20 or 2 bins, for ^{235}U we see differences up to 0.017% at the lower energy limit (2.25 keV) and up to 0.001% at the upper energy limit (25 keV); **the results are essentially indistinguishable.**



Using 20 or 2 bins, for ^{238}U we see differences up to 0.328% at the lower energy limit (20 keV) and up to 0.005% at the upper energy limit (near 149 keV); there is a small difference at 20 keV and virtually none at 149 keV. There is little significant difference that affects integral results (which help to explain why we saw no significant difference above for the K_{eff} values).



That is not to say that there is anything wrong with the 20 bands and it gives good answers, but for this application 20 bands simply isn't needed; **2 bands are sufficient as long as these 2 band parameters are defined using the multiband definitions to exactly conserve important moments of the flux, as I have done above; AS WITH ANY DISCRETE QUADRATURE, SUCH AS LEGENDRE QUADRATURE USED BY S_n CODES, THAT IS THE KEY.**

If both give the same results, does this means PTM and MB are equivalent? **Please do not make the mistake of assuming they are equivalent, because they ARE NOT.** Also, please do not make the mistake of assuming that PTM and MB results will always agree so closely that their

integral results are essentially indistinguishable, as we found in the above example here. In the above example they both produce statistically identical answers, only because they both used the same approximations.

What the above results show is that in this case the 2 band MB results using only moments from the PTM data, reproduce the 20 band PTM results. In other words, **we do not need 20 bands** to reproduce the rather small changes in the self-shielded cross sections that we see in these cases, i.e., only 4.6% for ^{235}U and 12.3% for ^{238}U .

This does not mean the two methods are equivalent, because PTM uses a number of approximations that MB does not. **In general MB can do much better than this because if we consider all the approximations used by PTM,**

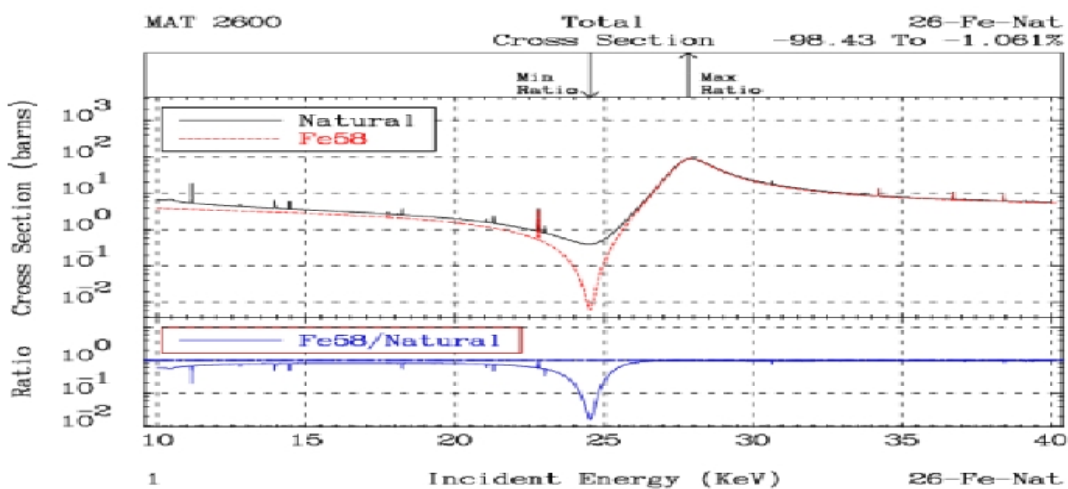
- 1) MB only needs moments of the cross sections, so there is no statistical uncertainty due to random sampling of a ladder of sampled resonances [5, 6].
- 2) By only using moments MB is not restricted to the ENDF restriction to SLBW [1].
- 3) MB uses the intermediate resonance [27, 28, 29], approximation, not the NR used by PTM [13].
- 4) MB uses an analytical solution to define the band weights and cross sections [12].
- 5) MB only uses a few cross sections bands, making practical an extension to deterministic codes, while still satisfying the all-important boundary conditions [14, 15].
- 6) PTM has only been applied to the unresolved region, whereas MB has been applied across the entire incident neutron energy range [10, 11]; in TART, from 1.0×10^{-5} eV to 20 MeV.

Bondarenko Model

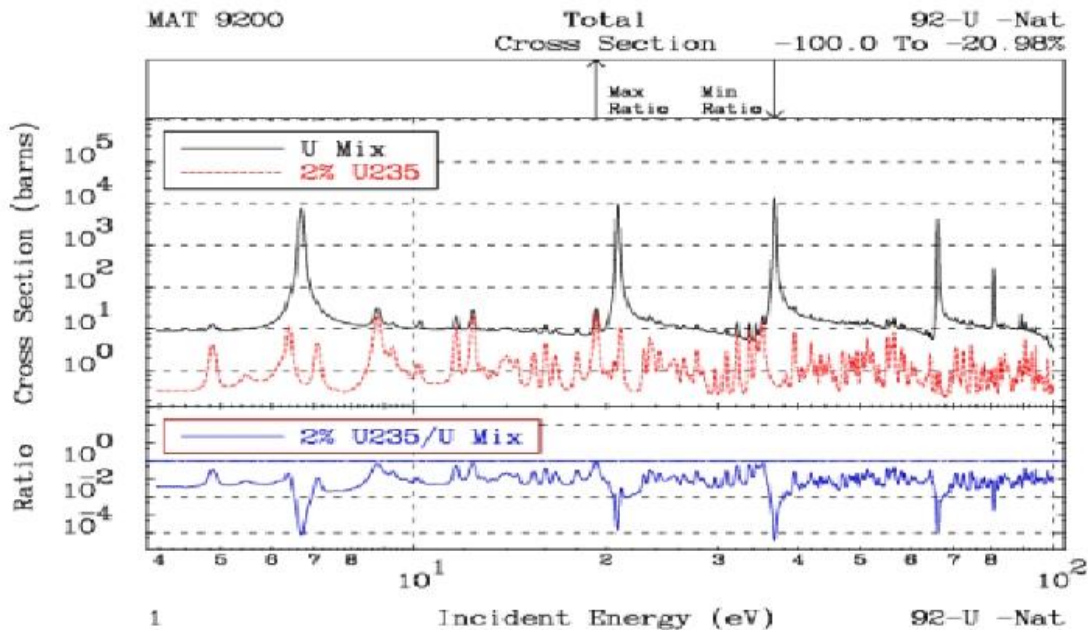
One additional approximation that both PTM and MB use is the Bondarenko approximation, that assumes the resonance structure in each isotope is independent of the resonance structure in all other isotopes; this predicts self-shielding of any mixture of isotopes as $1/[\Sigma_t(E) + \langle \Sigma_0 \rangle]$; $\langle \Sigma_0 \rangle$ represents all other materials. In principle this is an APPROXIMATION strictly valid only for **infinite, homogeneous** media, i.e., $\mu K = 0$. In practice, many years of use have proven how accurate it can be.

As applied here it means that when dealing with a mixture of isotopes, both PTM and MB sample the cross sections for each isotope, assuming the resonance structure in each isotope is independent of the resonance structure in all other isotopes. By the definition of “unresolved” that is about the best we can do in the URR. Although I doubt if it is of much importance in the unresolved region, I will merely mention that both PTM and MB cannot account for this effect and as such both are using the Bondarenko approximation. However, when used outside the unresolved energy range we can account for this correlation, in multi-group calculations, e.g., for N cross section bands, an N x N matrix of bands can include conditional probabilities, accounting for “coincidental” correlation. Here we see a BIG, important difference between using PTM with 20 cross section bands, and MB with only 2 bands. A MB 2 x 2 correlation matrix is easy to construct and understand, whereas a PTM 20 x 20 matrix really isn’t practical to even consider trying to construct or use.

The below figure compares the TOTAL cross section of Natural Iron (Fe) to the TOTAL cross section of Fe’s most abundant isotope, Fe56 (over 91% by atom fraction). Near the 25 keV window in Fe we can see that even though based on atomic fraction Fe56 is dominant, in terms of TOTAL cross section it is only about 1% of the Natural Fe TOTAL cross section. Hopefully this one figure will help you to appreciate, the magnitude of the APPROXIMATION of assuming that when defining self-shielded cross sections for Natural Fe, as an independent sum over its isotopes, for Fe56, we are assuming that the Natural Fe TOTAL can be APPROXIMATED by the Fe56 isotope TOTAL plus some constant $\langle \Sigma_0 \rangle$.



The below figure shows a comparison of the TOTAL cross sections for the Uranium mixture used in the above Simple 1-D model; the Uranium was 2% ^{235}U and 98% ^{238}U . The below figure shows an expanded view of the 4 eV to 100 eV energy range. We see a number of strong, widely spaced ^{238}U resonances (again, 98% of the mix), and more numerous ^{235}U resonances (only 2% of the mix). Here we can see examples of “coincidental” correlation, where rather than sitting on an energy independent $\langle \Sigma_0 \rangle$, the ^{235}U resonances are within the energy range of the strong ^{238}U resonances. From the ratio included in the below figure we can see a number of cases where a $1/\Sigma_0(E)$ weighting drastically changes the contribution of some ^{235}U resonances.



While the Bondarenko approximation has been successfully used for many years to produce processed nuclear data “application independent libraries”, today our modern evaluations have so much detail, including thousands and thousands of resonances, there are bound to be groups (ranges of energy) where there is what I refer to as “coincidental” correlation, where resonance just happen to rise or fall in similar patterns. Today our computers are so fast and large and efficient that we really no longer need to use the Bondarenko approximation, e.g., if you want to calculate the self-shielded cross section for any mixture of materials, we now have the computer resources to first define the total cross section of the mixture (e.g., use PREPRO/MIXER [7]) and then use this total as the self-shielding factor to calculate self-shielded cross sections for the individual constituents (use GROUPIE [7]); we need not construct tables of results for a variety of $\langle \Sigma_0 \rangle$; **we can bypass the Bondarenko approach and directly calculate one, unique answer.**

One method successfully used by TART for many years uses MB parameters over the entire energy range, usually 10⁻⁵ eV up to 20 MeV; not just the unresolved region. Many years of testing and comparison to TART continuous energy cross section treatment, shows that generally only 2 MB bands are needed to account for self-shielding. I mention this here because one the biggest problems with deterministic codes today is accounting for spatial and directional dependent self-

shielding. Over decades deterministic codes have used more and more groups to account for self-shielding; generally, this approach does not work, e.g., ^{238}U would require many thousands of groups and the group-to-group transfer matrix becomes of questionable use/accuracy. **What does work is fewer groups, but 2 cross section bands ala MB in each group.** This is a very practical approach as it can be even more efficient because you will find that you do not need nearly as many groups as you think you do.

Both PTM and MB use a rationale, Pade, approximation [14, 15], as the ratio of two polynomials to define the self-shielded cross section as a smooth continuous function over the entire range of $\Sigma_0 = 0$ to ∞ . This can be used to replace the somewhat crude methods used to interpolate in Σ_0 in tables of Bondarenko self-shielded cross sections. Here you will find that you need fewer values of Σ_0 to tabulate data, and results will be smooth and continuous.

$$\langle \Sigma_R(\Sigma_0) \rangle = \frac{\sum_B \Sigma_{RB} P_B / [\Sigma_t + \Sigma_0]}{\sum_B P_B / [\Sigma_t + \Sigma_0]}$$

The Intermediate Resonance (IR) Approximation

The **Probability Table Method** (PTM) uses the **Narrow Resonance** (NR) Approximation to sample from the entire distribution of cross sections after each scatter, so it is important for us to understand what this means and how it affects results. Here I will briefly describe the various resonance models, including Narrow (NR), Wide (WR), and Intermediate (IR), and investigate what effect these models have on our calculated results, and more importantly I will try to explain why. Returning to the 1-D Boltzmann equation,

$$\mu \partial \Phi(E, z, \mu) / \partial z + \Sigma t(E, z) * \Phi(E, z, \mu) = R(E, z, \mu) = R(E, z, \mu) \text{ is the slowing down and sources.}$$

In an infinite, homogeneous medium this becomes,

$$\begin{aligned} \Sigma t(E) * \Phi(E) &= R(E) \\ \text{Total Reactions} &= \text{Slowing Down Spectra} \end{aligned}$$

In the **Narrow Resonance** (NR) Approximation we assume that $R(E)$ is smoothly varying with energy, e.g., at successfully higher energies $R(E)$ is: Maxwellian, $1/E$, fission, and fusion spectra. Obviously, since we assume $R(E)$ is smoothly varying with energy, this equation says that the **Total Reaction Rate is smoothly varying**, and that the Flux $\sim 1/\Sigma t(E)$, the classic self-shielding I have been discussing throughout this paper.

In the other extreme the **Wide Resonance** (WR) Approximation we assume that the slowing down varies following the cross section,

$$\begin{aligned} \Sigma t(E) * \Phi(E) &= \Sigma t(E) * R'(E) \\ \text{Total Reactions} &= \text{Slowing Down Spectra} \end{aligned}$$

This equation says that the **Flux is smoothly varying**, and that the Flux is not self-shielded.

Briefly, the **Narrow Resonance** (NR) model assumes that the widths and spacings of the resonances in the medium are narrow compared to the range of secondary scattered energies, so there is a probability that the neutron can “see” the entire range of cross sections. In the other extreme of **Wide Resonance** (WR) model assumes that the resonance, or energy dependence of the cross section is so wide compared to the range of scattered energies that after a collision the neutron “sees” only the same cross section it saw before the collision.

In nature, when we examine the entire periodic table, we find almost a continuum of isotopes with various atomic weights, and resonance spacings and widths, that neither the narrow and wide model is accurate in all cases; hence the need for the **Intermediate Resonance** (IR) model. A detailed description of the IR is beyond the scope of this paper; see the papers by Rubin Goldstein [27, 28, 29]. Soon after developing the Multi-Band model [10,11, 12], I realized that based on the many results we were calculating, the NR is not always accurate enough, so I extended the multi-band method by adding the IR Approximation to TART [13]. Here I will merely present a few example results based on the six cross section models used above and adding IR results (identified as Multi-Band NR and IR) in the results.

Note that when using **Continuous** energy cross sections none of these resonance width models/approximations are used, so we can use continuous energy results as a standard to determine which of these models are accurate – or inaccurate.

Infinite, Homogeneous Model: The first example should be the simplest possible, corresponding to the above equation for an infinite, homogeneous medium. I homogenized the Water/U system discussed above, for a range of ratios of H₂O **molecules** to U **atoms**, including five different ratios: 1:100, 10:100, 100:100, 1000:100, 10000:100, i.e. from predominately U (100 times more), to predominately H₂O (100 times more). In each case I first used continuous energy cross sections and adjusted the ²³⁵U enrichment to make the system approximately critical. I then ran TART using each of the six cross section models discussed above, plus a seventh model to provide multi-band results using either narrow (NR) or intermediate (IR) resonance treatments. Each TART run used 10⁺⁸ neutron samples, to achieve converged results to within about 0.1% (3-digit convergence).

Infinite, Homogeneous: H₂O Molecules Atoms Ratio

| Model | 1:100 | 10:100 | 100:100 | 1000:100 | 10000:100 |
|---------------|----------|----------|----------|----------|-----------|
| Continuous | 0.999816 | 1.000080 | 1.000810 | 0.999657 | 1.000290 |
| Multi-Group | 0.966235 | 0.828187 | 0.794985 | 0.903417 | 0.987059 |
| Multi-Band NR | 1.000680 | 1.010940 | 1.023410 | 1.007310 | 0.999690 |
| Multi-Band IR | 1.000950 | 1.002020 | 1.000550 | 0.997719 | 0.998776 |
| Unshielded | 0.966169 | 0.828150 | 0.795056 | 0.903405 | 0.987063 |
| Totally | 0.999059 | 1.006050 | 1.090950 | 1.067940 | 1.027070 |
| Partial | 0.986059 | 0.935382 | 0.956772 | 0.997413 | 1.012270 |

Frankly I was shocked by the results; here is a summary of what I see from the above table,

- 1) The effects of the difference in self-shielding models are **most extreme near the middle of the table (100:100 ratio)**. For a much lower ratios the system becomes so heavily absorbing it is hard to see the effect of elastic scatter in the resonance range, and at much higher ratios the scatter is predominately from the water, particularly H, which scatters over such a large secondary energy range that it satisfies the narrow resonance (NR) model.
- 2) **Multi-group** and **Unshielded** results show incredible (at least to me), poor results; in the worst case predicting $k_{\text{eff}} \sim 0.795$, which is dangerously low if you are trying to predict the safety of a homogeneous mixture of materials; this result I found particularly surprising and SCARY!!!! Statistically these two models should – and do – produce very similar results; these results were so shocking I would not have believed them without this independent agreement.
- 3) **Totally** and **Partially** Shielded, respectively over (Totally ~ 1.091) and under (Partially ~ 0.956) results.
- 4) In this case the **Multi-Band Narrow Resonance** (NR) results are even worse than the Totally or Partially shielded results (NR ~ 1.023); not surprising, since U is does not satisfy the Narrow Resonance model.
- 5) Only the **Multi-Band Intermediate Resonance** (IR) results produce close to acceptable results across all five H₂O to U ratios (at 100:100 ~ 1.0005).

Simple 1-D Planar Infinite Model: The below table is identical to Table 1 above, under a Simple 1-D Planar model, except that I have added Intermediate Resonance (IR) approximation models. In this case the difference between narrow resonance (NR) and intermediate resonance is only 0.000320 (~ 0.03 %), which is insignificant to the statistical accuracy of the results. **The bottom line is that for this simple 1-D model NR versus IR plays no significant role.**

U/Water Criticality Including Narrow (NR) and Intermediate (IR) Results

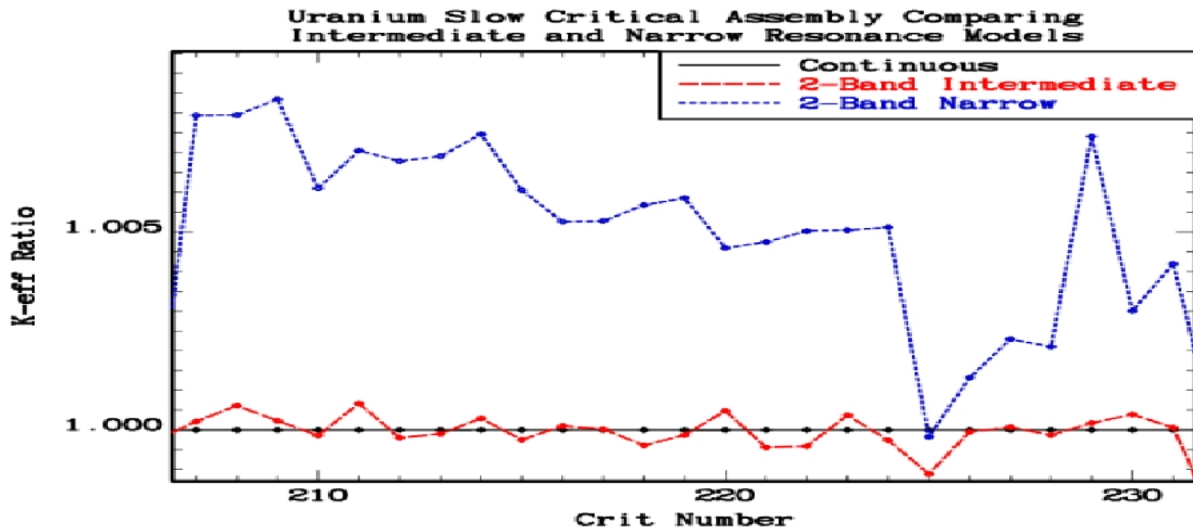
| Cross Section Representation | Expected K-eff | Difference in K-eff | Removal Lifetime (Microsec.) | Median Energy (eV) | Seconds |
|------------------------------|-----------------|---------------------|------------------------------|--------------------|----------|
| Continuous | 0.999924 | ----- | 7.89162D+01 | 5.00948D-02 | 5066.660 |
| Multi-Group | 0.974683 | -0.025241 | 7.70376D+01 | 5.01225D-02 | 3837.700 |
| Multi-Band NR | 1.000980 | 0.001056 | 7.90684D+01 | 5.01097D-02 | 4404.120 |
| Multi-Band IR | 1.001300 | 0.001376 | 7.90471D+01 | 5.00872D-08 | 4208.120 |
| Unshielded | 0.974645 | -0.025279 | 7.70372D+01 | 5.01247D-02 | 4442.640 |
| Totally Shielded | 1.001750 | 0.001826 | 7.97356D+01 | 4.95769D-02 | 4581.800 |
| Partial Shielded | 0.991570 | -0.008354 | 7.86170D+01 | 4.98773D-02 | 4512.280 |

Homogeneous versus Heterogeneous: Why is there such a significant difference between the preceding H₂O/U infinite, **homogeneous** system, and this H₂O/U finite, **heterogeneous** system? Because in the **homogenous** case the scatter was occurring in the entire uniform mix of materials, so that for some H₂O/U ratios the scatter from the U was important but did not satisfying the narrow resonance (NR) model. In the **heterogeneous** case the scatter and slowing down was primarily in the H₂O, which does satisfy the NR model. In the heterogeneous case what is important is not the scatter within the U, but rather the all-important boundary conditions at the H₂O to U interface; here the spectrum of neutrons incident from the H₂O into the U is smooth from scatter in H₂O and satisfies the narrow resonance model (NR).

The **Probability Table Method** (PTM) [24, 25], using the narrow resonance (NR) model in the unresolved resonance region has been more successful than you might think, even though most heavy even-odd isotopes (fuels), themselves do not narrow resonance (NR) scatter. As long as it is dealing with heterogeneous media where the slowing down is primarily outside of the fuel what is most important is not the scatter inside the fuel, but rather the boundary conditions to introduce neutrons into the fuel with the “correct” distribution of cross sections; hopefully this is illustrated by the above figures showing the energy and spatial dependence of the uncollided flux into the U from the H₂O.

The above two examples are for infinite homogeneous and heterogenous media, which being infinite are of course completely theoretical. To illustrate the differences between Narrow and Intermediate Resonance Models for real systems, below I present results for the Uranium Slow Critical Assemblies where using the Narrow Resonance Model we found small, but significant, differences for assemblies 207 through 231.

Uranium Slow Critical Assemblies: Below is a comparison for the Uranium Slow Critical Assemblies 207 through 231. These are the assemblies where we found significant differences using the Narrow Resonance (NR) Model; below the Narrow Resonance (NR) results are compared to Intermediate Resonance (IR) Model results. The results show that for these assemblies using the Intermediate Resonance (IR) reduces the difference to within 0.1%, except for one case (225) where it is 0.11% (statistically the same as 0.1%).



| Critical Assembly | Intermediate Resonance | Narrow Resonance |
|--------------------------|------------------------|------------------|
| 207 LCT006-1 U235 Water | 207 1.0002102 | 207 1.0079426 |
| 208 LCT006-2 U235 Water | 208 1.0006123 | 208 1.0079456 |
| 209 LCT006-3 U235 Water | 209 1.0002300 | 209 1.0083485 |
| 210 LCT006-4 U235 Water | 210 0.9998600 | 210 1.0060991 |
| 211 LCT006-5 U235 Water | 211 1.0006700 | 211 1.0070495 |
| 212 LCT006-6 U235 Water | 212 0.9998001 | 212 1.0067855 |
| 213 LCT006-7 U235 Water | 213 0.9999000 | 213 1.0069066 |
| 214 LCT006-8 U235 Water | 214 1.0002898 | 214 1.0074652 |
| 215 LCT006-9 U235 Water | 215 0.9997503 | 215 1.0060522 |
| 216 LCT006-10 U235 Water | 216 1.0000999 | 216 1.0052534 |
| 217 LCT006-11 U235 Water | 217 1.0000200 | 217 1.0052721 |
| 218 LCT006-12 U235 Water | 218 0.9996105 | 218 1.0056730 |
| 219 LCT006-13 U235 Water | 219 0.9998701 | 219 1.0058548 |
| 220 LCT006-14 U235 Water | 220 1.0004792 | 220 1.0045922 |
| 221 LCT006-15 U235 Water | 221 0.9995608 | 221 1.0047417 |
| 222 LCT006-16 U235 Water | 222 0.9995907 | 222 1.0050217 |
| 223 LCT006-17 U235 Water | 223 1.0003694 | 223 1.0050425 |
| 224 LCT006-18 U235 Water | 224 0.9997404 | 224 1.0051126 |
| 225 LMT001 U-nat D2O | 225 0.9988893 | 225 0.9998243 |
| 226 LMT002-1 U235 D2O | 226 0.9999504 | 226 1.0013182 |
| 227 LMT002-2 U235 D2O | 227 1.0000700 | 227 1.0022889 |
| 228 LMT002-3 U235 D2O | 228 0.9998713 | 228 1.0020988 |
| 229 LMT002-6 U235 D2O | 229 1.0001731 | 229 1.0074080 |
| 230 LMT002-10 U235 D2O | 230 1.0003893 | 230 1.0030043 |
| 231 LMT002-11 U235 D2O | 231 1.0000580 | 231 1.0041909 |

Nuclear Data Section
International Atomic Energy Agency
Vienna International Centre, P.O. Box 100
A-1400 Vienna, Austria

E-mail: nds.contact-point@iaea.org
Fax: (43-1) 2600
Telephone: (43-1) 2600 21725
Web: <http://www-nds.iaea.org>
